

Spent fuel corrosion and dissolution

R S Forsyth¹, L O Werme²

¹ Studsvik AB, Nyköping, Sweden

² Swedish Nuclear Fuel and Waste Management Co,
Stockholm, Sweden

December 1991

SPENT FUEL CORROSION AND DISSOLUTION

R S Forsyth¹, L O Werme²

1 Studsvik AB, Nyköping, Sweden

2 Swedish Nuclear Fuel and Waste Management Co,
Stockholm, Sweden

December 1991

Information on SKB technical reports from
1977-1978 (TR 121), 1979 (TR 79-28), 1980 (TR 80-26),
1981 (TR 81-17), 1982 (TR 82-28), 1983 (TR 83-77),
1984 (TR 85-01), 1985 (TR 85-20), 1986 (TR 86-31),
1987 (TR 87-33), 1988 (TR 88-32), 1989 (TR 89-40)
and 1990 (TR 90-46) is available through SKB.

SPENT FUEL CORROSION AND DISSOLUTION

R.S. Forsyth, Studsvik AB, S-611 82 Nyköping, Sweden*

L.O. Werme, Swedish Nuclear Fuel and Waste Management Co., Box 5864, S-102 48 Stockholm, Sweden.

* Present address: CALEDON-CONSULT, Stenbrinken 7, S-611 34 Nyköping.

ABSTRACT

This paper presents the current status of the Swedish programme for the study of the corrosion of spent fuel in bicarbonate groundwaters. Results from the on-going experimental programme are presented and compared with the data base accumulated over the past ten years. Release of uranium and the other actinides was solubility-controlled under the semi-static type of experiments performed. The limiting solubility for uranium under oxic conditions was consistent with the hypothesis that the redox potential of the system is assumed to correspond to the U_3O_7/U_3O_8 transition. The measured release fractions for ^{137}Cs , ^{90}Sr and ^{99}Tc are discussed and used to exemplify the probable dissolution and corrosion processes involved. A substantial part of the Swedish programme is directed to the characterization of spent fuel before and after corrosion tests. Recent results are presented on the identification of possible corrosion sites.

1. Introduction

The direct disposal of spent nuclear fuel is a route in high-level waste management favoured by several countries, such as the U.S., Canada, Sweden, Finland and Spain. Common to the methods proposed for the safe, permanent disposal of spent reactor fuel is the concept of multiple barriers to radionuclide release to the biosphere. The outermost barrier is a suitable geological formation, where the encapsulated waste will be buried at a depth of several hundred meters. The innermost barrier is the limited solubility or dissolution rate of the ceramic UO_2 fuel itself and of the radionuclides embedded in the fuel matrix. Studies of the dissolution of spent fuel in groundwater started in the late 1970's [1,2,3], and since then some thirty papers have been published on the subject, mostly in symposia proceedings or as laboratory reports [4,5,6,7,8]. A recent overview of the work performed on spent fuel as well as on unirradiated fuel has been published by Johnson and Shoosmith [9].

This paper is a status report on the Swedish programme with emphasis on recent results in which their evaluation is performed against the background of the data-base accumulated throughout the whole experimental programme. In particular, results from the characterization of spent fuel before and after corrosive attack are now becoming available and these will be discussed here. Some preliminary results from these studies have already been reported [10,11] but not in a comprehensive form. An update of the actinide release data, together with a comparison with results obtained in other laboratories performing similar experiments, will also be presented.

2. Experimental

2.1 Fuel

Most of the corrosion experiments performed to date have used 20 mm long segments of fuel and clad, or fuel fragments from two reference rods: rod 418-A6 from the Oskarshamn 1 BWR and rod D07/B15 from the Ringhals 2 PWR. The rods had maximum burnups of 42 and 43 MWd/kgU, respectively. Fuel specimens were dry-cut from two different locations in the rods near the maximum burnup positions. The rods were selected for the corrosion test programme on the basis of their burnup level and their integral fission gas release values of 0.7 and 1.06%, respectively. Thus the rods were not subjected to significant thermal feed-back effects during the irradiation and were therefore fairly representative of the bulk of discharged fuel in the Swedish power reactor programme.

Two years ago, an additional BWR rod was included in the experimental programme in order to study the effects on corrosion of burnup/linear power. Rod 79B2 was the bottom segment of a stringer rod irradiated for 8 cycles in the Ringhals 1 BWR. The local burnup along the fuel column, excluding the end-pellets, varied between 21 and 49 MWd/kgU, and only during the first irradiation cycle did the maximum-rated pellet experience a linear power as high as 25 kW/m. Fuel/clad specimens were dry-cut from different burnup positions along the rod and subjected to corrosion testing.

The choice at the inception of the programme of fuel/clad segments for most of the corrosion tests was based on the requirement that the fuel specimens used should be as representative as possible of the discharged fuel, i.e. that a whole cross-section of the fuel, with its radially-varying properties and the clad itself with possible fission product deposits, should

be exposed to the leachant. Additional advantages with the use of fuel/clad segments are that leachant access to the fuel surfaces is comparable to the real case. Additional analytical complications due to fuel fines and dust are reduced although not entirely eliminated. Fuel fragments have been used occasionally in order to assess the effect of fuel fragment size on corrosion properties, or, for well-defined fragments, to investigate the possibility that certain fuel zones are subject to preferential attack.

2.2 Leachants

Two water types, a synthetic groundwater (Table 1) and deionized water, have been used in the experimental programme, although occasionally with adjustments to pH or bicarbonate content. Deionized water was only used in selected experiments, partly for comparison with other programmes, and it was always purged with nitrogen prior to use in order to minimize the carbon dioxide content.

2.3 Experimental procedure

The specimen, a fuel/clad segment suspended in a spiral of platinum wire or fuel fragments in a platinum dish, was immersed in 200 ml of leachant in a 250 ml Pyrex flask. All tests were performed at 20-25°C, the ambient temperature of the hot-cell. After completion of each contact period, the specimen was removed and the test terminated or the specimen was transferred to a new flask with new leachant. Several 10 ml aliquots of leachant were centrifuged through membrane filters with nominal apertures of 1.2-2.0 nm (Amicon Corp. USA). The empty Pyrex flasks, after a rapid rinse with distilled water, were

stripped of possible adsorbed material (and fuel fines) by exposure for a few days to 5M HNO₃/0.5M HF. All 3 fractions, centrifugate, membrane filter and vessel strip solution, were analyzed.

Rather surprisingly, no conclusive evidence of significant amounts of colloidal or adsorbed actinide species has been obtained from the analytical results on over 200 membrane filters and strip solutions, with some reservations in the case of ²⁴⁴Cm. Cesium and strontium nuclides, however, were shown to be retained on the membrane filters, under both oxidizing and reducing conditions, to the extent of 5% and 12% respectively in groundwater, and 16% and 66% in deionized water. Successive centrifugations of the same leachant through new filters showed that these values were roughly the same on each centrifugation. Appreciable adsorption of cesium and to a lesser extent strontium nuclides on the leachant vessel was also observed in experiments of long duration. The fraction of the total release thus adsorbed being dependent on residence time and not on molar concentration. The total release values reported for these nuclides include the contributions mentioned above.

Most experiments have been performed with 50 ml of air above the leachant, but data has also been obtained for anaerobic conditions. Such conditions have been created by three different methods: 1) by performing the experiments under an argon atmosphere, 2) using synthetic groundwater which had been reduced by circulation over crushed bore-cores, and 3) by having a palladium black catalyst present in the solution. None of these experiments were instrumented.

2.4 Analysis

Elemental analysis was performed by laser fluorescence for uranium, α -spectrometry for plutonium and curium, γ -spectrometry for the major γ -emitting fission products and radiochemical separation and β -counting for ^{90}Sr and ^{99}Tc . For strontium, technetium and molybdenum optical emission ICP was also used.

3. Corrosion tests: actinides

The results for the actinide releases obtained within these experimental series are similar. It is therefore instructive to discuss also the results obtained within research programmes other than the Swedish programme. The tuff groundwater used in the US Yucca Mountain programme and the Swedish granitic groundwater are similar; both are bicarbonate type groundwaters with low chloride content and data obtained in the Yucca Mountain Program are of particular interest for comparison with Swedish data.

The US and Swedish studies were performed on light water reactor fuel (PWR and BWR) of higher burnup; in the US programme 30 MWd/kg U and in the Swedish program slightly over 40 MWd/kg U. The differences in burnup have an impact on the fuel inventories of plutonium and neptunium. In a very low burnup fuel, ^{239}Pu dominates while other plutonium isotopes grow in with increased burnup.

3.1 Uranium

The concentrations obtained for uranium in both groundwater (2 mmol/L HCO_3^-) and deionized water are shown in Figure 1. The

data are plotted against cumulative contact time. Over the first week of contact, the concentration increases to $4 \cdot 10^{-6}$ mol/L and remains constant at that level for 500 days. At longer cumulative contact times, there is a slow increase in concentration and after some thousand days, the concentration is $2 \cdot 10^{-5}$ mol/L. In the Yucca Mountain Project, the average concentrations were $6 \cdot 10^{-6}$ mol/L (series 2; fused silica leach vessels [12]) and $1.3 \cdot 10^{-6}$ mol/L (series 3; stainless steel leach vessels [13]). The cumulative contact times were in the range of 500 to 1,000 days. Thus, the data are in good agreement with our data for the comparable cumulative contact times.

For deionized water, the uranium concentrations are considerably lower. There is also a wide spread in the data, with an average of $6 \cdot 10^{-8}$ mol/L. However, many of the data points plotted in Figure 1 are reported as less than values, which accounts for some of the apparent spread and also adds uncertainty to the value of the average concentration.

3.2 Plutonium

As for uranium, the plutonium concentrations in solution rapidly attain a constant value. The plutonium data obtained so far within the Swedish program are shown in Figure 2. The plutonium concentrations after short term exposures are relatively high, with a spread between 10^{-9} to 10^{-8} mol/L. At longer contact times, the concentrations drop and appear to level out at just below 10^{-9} mol/L. For deionized water the concentration remains high, independent of contact time with an average value of $1.3 \cdot 10^{-8}$ mol/L.

These data are compared in terms of fractional releases with the uranium fractional releases. For contact with groundwater,

the ratio between plutonium and uranium normalized releases is almost 10^{-2} for longer exposure times. For deionized water, the corresponding number is ~ 10 . This is due to a combination of higher plutonium concentrations and considerably lower uranium concentration in deionized water as compared to groundwater, where the complexation with carbonates results in an increase of several orders of magnitude in uranium solution concentrations.

The actinides are expected to be in solid solution with the UO_2 fuel and will be mobilized congruently with the oxidative dissolution of the fuel matrix. However, as discussed, the ratios between the release fractions show that the release of plutonium to the leachate is independent of the uranium release. This together with the observation that the solution concentrations are constant with time clearly indicate solubility control of the plutonium release. A comparison between plutonium concentrations from fuel corrosion experiments performed in groundwater are given in Table 2. In addition to LWR reactor fuel, data from leach experiments performed by CEA Marcoule on Phenix fuel has been included [14]. Phenix is a fast breeder reactor and the fuel studied had a plutonium dioxide content of ca 20 %. As can be seen in Table 2, there is a fairly good agreement between the data from the different laboratories, particularly in view of the different fuel types used for the studies. Even for a low burnup fuel (ca. 0.5 MWd/kgU), the steady state plutonium concentration is close to what is found for high burnup fuel despite the fact that the Pu content of this fuel is only ca. 1 % of that in the other fuels. Also for the fast breeder fuel, the Pu concentration is in fair agreement. For this experiment, no pH value was reported.

3.3 Comparison with calculations

Calculations using the EQ3/6 code [15] (version 0288) have been performed in order to determine if the steady state actinide concentrations observed under oxidizing conditions could be related to solubility control by a precipitated actinide phase. The thermodynamic data base for uranium was the SKBU1 [16]. For plutonium the data base provided with the code package had been modified as discussed by Puigdomènech and Bruno [17]. The most stable phases that may form in the uranium-groundwater system are uranyl silicates. However, it is probable that schoepite formation is the kinetically favoured secondary phase. Calculations using the EQ3/6 code for a system with $p_{O_2} = 0.2$ atm predicts higher uranium concentrations in solution by at least a factor of 10. Even though there is a rather wide spread in the uranium concentration data, no measurement as high as predicted has been recorded. Also for neptunium, high concentrations are predicted, much higher than are observed in the Yucca Mountain Project [12, 13]. Neptunium concentrations have not yet been measured in the Swedish programme.

The experiments have been performed with air present. At the same time the predominant oxidation state of uranium in the solid phase is +4. Hence, the system is not at equilibrium, a fact that makes it difficult to use equilibrium codes for the calculations of speciation in the solution phase. In order to handle this problem we have used the following reasoning: The uranium oxides UO_{2+x} are semiconductors with a noticeable electric conductivity. Thus, the UO_{2+x} phase can be considered as a redox buffer, which has a much larger buffering capacity than the solution/gaseous phase. The redox potential for systems with $0 < x < 1$ is much lower than the redox potential calculated from the partial pressure of O_2 . Solubility calculations were performed assuming that the redox potential is determined by

the transitions between various UO_{2+x} phases. The results obtained for the U_3O_7/U_3O_8 equilibrium are presented in Figures 3 to 5 together with data from experiments performed at different pH values. As shown in Figures 3 to 5, there is a quite good agreement between the calculated solubilities and the measured data. At low pH values, the agreement is less good. However, these experiments had a short duration (ca. 20 days), and equilibrium might not yet have been attained.

The neptunium data indicate that if there is a solubility control, the solid phase must be a Np(IV) phase. If Np(V), most probably NpO_2OH , controlled the solubility, the solution concentration would have been in the millimolar range.

The plutonium solubilities are not redox sensitive within the range of redox potentials relevant for the experiments. Thus, the Pu data neither supports nor contradicts the hypothesis that the solution concentrations are controlled by the U_3O_7/U_3O_8 redox potential. However, the data base used for the EQ3/6 calculations fails to explain the difference of over one order of magnitude in Pu concentrations in groundwater and DIW. At lower pH, the differences between calculated solubilities and measured concentrations becomes quite large. However, the uranium and plutonium ratio in solution is close to that in the fuel itself. This indicates that the plutonium most probably is not in equilibrium but controlled by the uranium dissolution.

4. CORROSION TESTS: FISSION PRODUCTS

Certain individual fission product nuclides, such as ^{99}Tc , ^{129}I and ^{135}Cs , are of specific interest for safety analysis because of a combination of factors such as radiological toxicity, fission yield, half-life and water transport through the buffer

and rock zones surrounding the waste package. Safety analysis must consider the fate of other fission products with shorter half-lives when one considers the scenario of a possible early canister failure caused by, for example, manufacturing defects.

The release of the actinides, including uranium, is solubility-limited, and hence measurements of their concentration in solution under the experimental conditions cannot yield quantitative measures of the on-going dissolution process or processes. Here, it is useful to measure the release of one or more fission products which are monitors of the corrosion rate of the fuel matrix. This requires that fission product "monitors" be homogeneously distributed throughout the fuel and that their solubilities in the leachant be sufficiently high so that solution saturation is not attained. Obvious candidates as corrosion "monitors" are the rare-earth fission products which are formed with high fission yield and form solid solutions with UO_2 . However, their release to the leachant is subject to the same solubility constraints as the actinides. Thus, extensive measurements of fission product release have been performed. There is now a good understanding of the various processes involved in the corrosion and dissolution of spent fuel and in the selective release of certain fission products. There is still, however, some uncertainty in the definition of matrix dissolution by means of a fission product "monitor", as the currently favoured candidate, ^{90}Sr , appears on the basis of some measurements to be enriched at the grain boundaries.

4.1 Cesium, Strontium and Technetium

Under oxic conditions, these three elements together with iodine, which will not be considered further here since its

release data is not as extensive as for the others, are fairly readily solubilized. However, the variation of their release behaviour as a function of time show such differences that at least partly different release mechanisms are indicated.

4.2 Cesium

For cesium and iodine, there is an abundant literature regarding its migration to grain boundaries, fuel surfaces and clad in operating reactor fuel. At higher values of linear power the release has been shown in numerous studies to be closely correlated to the release of the fission gases krypton and xenon. Thus, in the first few weeks of contact between spent fuel and water, there is a rapid solubilization of cesium nuclides, the so-called "Instant Release Fraction". This is illustrated in Figure 6 which presents release rate data for ^{137}Cs under oxidic conditions for fuel/clad segments from the three reference fuel rods in the Swedish Programme. The data plotted for the Ringhals-1 fuel rod, which contained fuel of burnup varying from 21 to 49 MWd/kgU, refers only to fuel specimens of burnup between 43.8 and 46.5 MWd/kgU, i.e., at about the same burnup level as the specimens from the other two rods. Data from tests in both the reference groundwater and deionized water are presented. There is no apparent difference between the ^{137}Cs release rates even though uranium concentrations in the leachants differed by two orders of magnitude. After the initial rapid release of the Instant Release Fraction, the release rates decrease fairly quickly but, with the data so far available, appear to level off with time. Note also that the Ringhals 1 fuel, with somewhat higher burnup and integral fission gas release, exhibits lower and less-steeply varying release than the other two reference fuels.

4.3 Strontium.

The corresponding data for ^{90}Sr release (Figure 7) show that during the first few weeks of water contact, the ^{90}Sr release rate is constant, before showing about the same decrease with time as the values for ^{137}Cs . There are appreciably less scatter in the data, such that all the measured values after the first month are included within a narrow envelope. At this stage, the slope is close to -1. The ^{90}Sr values are always lower than the corresponding values for ^{137}Cs . The statistical scatter in the results for both ^{90}Sr and ^{137}Cs is less than is apparent in Figures 6 and 7. As was mentioned above, the fuel/clad segments from both the Oskarshamn 1 BWR and the Ringhals 2 PWR fuel rods were cut out from different, but nearby, parts of the rod. Local differences in post-irradiation fuel characteristics were not expected over such short axial distances. However, there is an apparent correlation between the release rates for both ^{137}Cs and ^{90}Sr over the duration of the corrosion tests and the position of the specimen in the fuel rod. Figure 8 presents the cumulative release fractions of ^{90}Sr for the fuel/clad segments taken from the PWR rod. The odd- and even-numbered specimens, respectively, were taken from positions immediately adjacent to each other between the 3rd and 4th spacer grids, where time-varying power effects would be very similar. The burnups of the two groups was shown to be practically identical by measurement of the $^{134}\text{Cs}/^{137}\text{Cs}$ ratios on all leachant solutions. The mean value for the odd-numbered segments was 0.509 ± 0.006 ; for the even-numbered, 0.510 ± 0.007 .

Figure 8, however, shows a small but clear and persistent difference in the ^{90}Sr release rates between the two groups. Admittedly, the effect is a small one. Even after 5 years of cor-

rosion, with a fractional release rate of 10^{-7} /day and still decreasing with time, less than 0.1% of the ^{90}Sr inventory had been released to the leachant under (conservative) oxidic conditions. Modelling of spent fuel corrosion and dissolution must establish in the long term if these observed effects are indeed representative of a preferential corrosive attack at zones in the fuel enriched in ^{90}Sr , or whether the release rates in the later stage of Figure 7 represent matrix dissolution. If the latter alternative is true, a reasonable hypothesis is that the difference between the release behaviour of ^{137}Cs and ^{90}Sr (Figures 6 and 7) reflects only the migration of cesium during irradiation. The Instant Release Fraction (first few weeks), represents cesium released from the fuel grains to fuel/clad surfaces. The difference in the later stages of corrosion represent attack at grain boundaries (which slowly open) enriched in migrated cesium. Such cesium-enriched zones at the individual grain level have been demonstrated during the electron probe microanalysis (EPMA) examination of power-bumped fuel [18]. Whether similar strontium enrichment had occurred could not be determined due to imprecision in the measurements at these detection levels.

4.4 Technetium

The available data on ^{99}Tc release under oxidic conditions are presented in Figure 9. The measured release rates for the two reference Ringhals rods are in broad agreement, although with more scatter than was observed for ^{137}Cs and ^{90}Sr . Compared with these two nuclides, the presence of ^{99}Tc at or between the fuel grain boundaries in fission gas bubble sites has been well documented over the past quarter of a century. Metallic inclusions of Mo, Tc, Ru, Rh and Pd, usually, but not always, with a

composition corresponding to their respective fission yields, have been observed in zones of fuel cross sections determined by operating temperatures and burnup. The inclusion sizes observed by optical or scanning-electron microscopy are in the micron range, but Thomas et al. [19] have shown by transmission electron microscopy that spent PWR fuel contained inclusions down to sizes of tens of nanometers, the larger of which were located at or close to the grain boundaries. An estimate of the amount of such inclusions in the reference Oskarshamn 1 BWR and Ringhals 2 PWR fuel by dissolution and filtration [20] showed that 4.5 and 4.9 mg/g fuel, respectively, could be separated, of which 10 weight percent consisted of ^{99}Tc . The access of water through fuel cracks and networks of fission gas bubble sites to a fairly large technetium source term is thus relatively easy. The release of ^{99}Tc is probably controlled only by the oxidation of the inclusions. The release is maintained at a rate of between 10^{-5} and 10^{-6} /day, such that after a few years it exceeds those for ^{137}Cs and ^{90}Sr (Figure 9).

4.5 Reducing conditions

The data presented and discussed above were obtained from experiments conducted under oxidic conditions, which is a conservative case, since the deep-rock granitic groundwaters are known to be reducing. Although there are experimental difficulties in establishing and maintaining reducing conditions in a hot-cell environment for long periods, a number of uninstrumented corrosion tests have been performed on the reference fuels, where reducing or anoxic conditions have been imposed by the three methods described in the experimental section. The effects of anoxic conditions (pure argon environment) on fractional release from a series of fuel/clad specimens from the Ringhals-

1 BWR rod are illustrated in Table 3. Actinide solubilities have been discussed earlier in this paper and the release fractions are included here only as a comparison. The change in redox conditions has a major effect on the solution concentrations of ^{99}Tc , decreasing by two orders of magnitude, while only minor decreases in the cumulative release fractions were noted for ^{137}Cs and ^{90}Sr . The average ^{99}Tc concentrations under reducing conditions were found to be $6 \cdot 10^{-9}$ mol/L. This value is to be compared with a technetium solubility of $3 \cdot 10^{-8}$ mol/L, controlled by TcO_2 , which is the stable phase under the experimental conditions. The agreement is quite good. However, technetium was also present in the fuel in metallic form and more definite conclusions will have to await the results of further studies. For ^{137}Cs and ^{90}Sr a comparison of their release rates gives more information on the mechanisms involved (Tables 4 and 5). The release of ^{137}Cs during the first 21 days of corrosion is independent of redox conditions, confirming that the Instant Release Fraction consists of a readily-solubilized species. During this period the ^{90}Sr release rate shows a more marked difference between oxic and anoxic conditions, particularly during the second contact period, when the fractional release rate has already fallen below the 10^{-6} /day level. During the last contact period, the rates for both nuclides are below this level, even under oxic conditions, but at this stage ^{137}Cs release is more redox-dependent. For the first time, its release rate under reducing conditions is lower than the rate for ^{90}Sr , suggesting that corrosive attack occurred at sites already relatively depleted in ^{137}Cs , either during reactor operation or previous attack.

These observations are broadly confirmed by the results on the other fuels and with the other methods for maintaining reducing conditions, but at longer contact times, the ^{90}Sr release rate

is lower than that for ^{137}Cs . The initial release of Sr-90 under anoxic conditions may be mainly due to dissolution of fuel already partly oxidized, probably during air-contact prior to the tests, but that even at this stage, there is an underlying fractional release rate of the order of $5 \cdot 10^{-7}/\text{day}$. With the available data it is not possible to state which mechanism or mechanisms are responsible for this release.

5. Corrosion sites

It would be a major step forward in defining the mechanisms for spent fuel corrosion and dissolution if it could be experimentally established whether or not preferential attack occurs and whether the sites for such attack are dependent on fuel properties such as burnup and irradiation history. The Instant Release Fraction, of course, is dependent on these parameters, but as shown above, this appears to be independent of attack on the bulk fuel.

5.1 Fuel fragment corrosion tests

In order to undertake a more systematic search for possible corrosion sites, an experimental series was started at the end of 1985 in which selected fragments of fuel from the reference Oskarshamn 1 BWR rod were exposed to long-term contact with four different leachants. Three were modifications of the bicarbonate groundwater (Table 1) with identical compositions except for bicarbonate molarities which were 1.0, 2.0 and 4.0 mmol/L, respectively. The fourth leachant was deionized water. The groundwater with 4.0 mmol/L bicarbonate and the DIW, therefore, represented the extreme cases for uranium solubility.

The use of fuel/clad segments for corrosion tests meant that a representative cross-section of the fuel was exposed to the leachant. Sieving tests on the Oskarshamn 1 fuel, however, showed that 70 weight percent of the fuel was in the form of fragments larger than 4 mm. It was thus possible to select individual fuel fragments delineated by two radial fuel cracks and the pellet periphery which were approximately representative of the bulk fuel and also exposed well-defined fuel surfaces formed in the reactor to the leachant. The effects of radial variation in fuel morphology, possible evidence of local attack and formation of alteration products could be studied by examination of the fragments after completion of the corrosion tests. The burnup of the Oskarshamn 1 fuel used in the experiments was 41-42 MWd/kgU, and so, in addition to the usual peripheral enhanced α activity [20], the fuel was expected to show some development of the features of the fuel rim zone typical of high burnup: increased porosity and a marked change in grain size and morphology [21]. Hence, parallel with the corrosion tests on the fuel fragments, the reference fuel has been characterized with respect to these features.

Figure 10 shows the radial variation in fuel porosity, the Nd/U atomic ratio as determined by EPMA, and α activity measured by the photodensitometric scanning of an autoradiography film. The α activity distribution is plotted on an arbitrary scale, normalized to the activity at the pellet centre and refers only to the distribution some 10 years after discharge from the reactor and roughly half-way through the fragment corrosion tests. In contrast with porosity and burnup distribution, which are time-independent in spent fuel, the local α activity and nuclide composition is determined by both irradiation history and decay time. At shorter cooling times, the α gradient at the fuel edge is much steeper due to curium nuclides, in particular ^{242}Cm .

The fuel pellet rim, because of this combination of increased porosity and local α dose rate, is obviously a zone where preferential corrosive attack could occur. The enhanced burnup at the rim has been attained predominantly by fission of plutonium nuclides, whose fission yield curves show a marked increase in yield for Tc, Ru, Rh and Pd and a somewhat lower yield for a number of elements which forms oxides and remain in solid solution with the UO_2 , as compared with the case for fission of ^{235}U . This will have the effect of increasing the fuel's O/M ratio.

Studvik's SEM is only equipped with local radiation shielding, which does not permit the examination of whole fuel cross-sections. Instead, thin (0.2 mm) diametral strips, 1.5 mm wide are prepared from the cross-sections previously examined in the fully-shielded optical microscope. The cut sides of these fuel strips can be regarded as a continuous fracture surface so that both the as-polished fuel structure and the underlying morphology can be examined across the entire diameter. The characterization of the reference Oskarshamn 1 fuel included an examination and creation of a photomosaic of the as-polished rim zone which will be presented for comparison with corroded specimens. A systematic examination of the fracture surface with emphasis on the rim zone was also performed. At the periphery (Figure 11) the fuel displayed the same loss of grain structure reported by other workers [21,22,23]. Grain edges and faces, particularly at fission gas bubble sites (Figure 12), were decorated by spherical particles with a size of a few hundred nanometres. Whereas the high porosity zone in this fuel was only 30-40 μm wide, large populations of these small particles were observed in a zone extending 250 μm in from the rim and even inwards to a radial position of 4 mm, although with sharply reduced frequency. Attempts to identify this material by X-ray diffraction

examination (XRD) of small pieces of fuel rim have so far been unsuccessful, only the normal UO_2 pattern being observed.

Two of the fragment corrosion tests have been completed, experiment 3.25 (1427 days in the 4 mmol/L bicarbonate groundwater) and experiment 3.26 (1521 days in DIW). On removal from the leachant, fuel fragments from both tests were black, but the DIW-exposed fragments developed an almost uniform covering of yellow material within a few seconds after being placed beneath the in-cell lamp for periscopic examination. This deposit was identified by XRD as dehydrated schoepite of nominal composition $\text{UO}_3 \cdot 0.8\text{H}_2\text{O}$, which was also identified previously on the surfaces of a fuel/clad segment from the PWR reference rod which had been corroded in DIW [24]. The fragments may have been initially covered by a film of schoepite containing an excess of structural water, the amber form mentioned by Finch and Ewing [25]. This water was lost irreversibly by warming under the lamp.

A higher water/fuel ratio (200 g/g) was used than in the fuel/clad segment tests. Together with the free access of water to the fragment surfaces, this resulted in somewhat higher fractional release than observed with segments. The cumulative fractional release values obtained by solution analysis for the two experiments are presented in Table 6. Apart from the expected differences in uranium concentrations, the progress of corrosion has been comparable in the two tests. Note also that the cumulative fractional release of ^{99}Tc exceeds that for ^{90}Sr in both tests, confirming the relatively constant release rate for ^{99}Tc under oxidic conditions. After completion of the tests, specimens of the respective fuel fragments were prepared for SEM and EPMA examination. Here, however, the specimens were prepared so that one of the original fragment sides i.e., the

side of a radial fuel crack, could be inspected in addition to the pellet rim. Photomosaics of SEM images of the outermost rim zones of the uncorroded reference fuel and of specimens of the corroded fragments are presented in Figure 13. Corrosion, demonstrated by enlargement and interlinkage of the peripheral porosity, has occurred in this region, particularly in specimen 3.26, which had shown the largest release fractions of strontium. Note also the crystals of UO_3 hydrate which are visible at the fuel surface. Inspection of the fracture surfaces of the two corroded specimens showed that the small particles found in the reference material were still present. Although it is impossible to quantify their population densities, a visual assessment suggested that the corrosion process did not seem to have markedly decreased their number. The type of corrosion shown in Figure 13 was not found on the sides of the fragments away from the periphery, but there was an apparent enhancement of the frequency of grain pull-out during polishing of the corroded specimens as compared with the reference fuel. This effect is evident over the outermost millimeter of the fuel, coinciding with the zone in which the small particles at the grain boundaries had been observed.

The burnup at the rim of the Oskarshamn 1 fuel; as shown by the Nd/U ratio, was about 80 MWd/kgU; Bleiberg et al. [26], some 30 years ago, reported grain subdivision in UO_2 irradiated to this burnup. Inspection of the micrographs in Figure 12 shows clear evidence of a process of grain subdivision. The particles were predominantly observed at grain edges and corners, the sites of fission gas bubble precipitation, where the solid/gas interface experiences an enhanced deposition of energy from fission fragments and α particles during reactor irradiation at high burnup. This may initiate the recrystallisation of the UO_2 grains,

with an increased mobility and release of the fission gases and perhaps other fission products.

The changes in porosity and grain structure at the rim of high burnup fuel pellets are currently attracting a great deal of interest in a number of research centres and, hopefully, the studies now underway will lead to a much better understanding of the mechanisms involved. Meanwhile, the two remaining fuel fragment experiments have experienced over two more years of corrosion than the experiments described here. These experiments will be terminated in the near future, and systematic fuel examination programmes performed.

5.2 Effect of burnup/linear power rating on fuel corrosion properties

From these results, there are still a number of unresolved questions regarding the corrosion of spent fuel: a) the role of ^{90}Sr as a possible monitor of the on-going corrosion process; b) whether the observed small decrease in the release rate of ^{90}Sr under nominally reducing conditions is due to radiolysis effects or redox-independent processes; c) if radiolysis effects are significant, the definition of a relationship between dose and corrosion rate; d) whether corrosive attack is directly proportional to exposed surface area or whether preferential attack occurs. It is unavoidable that the observations from all experimental programmes using presently-available spent fuel are dominated by relatively short term effects, and it is therefore essential that a good understanding of these effects be attained in order to avoid the construction of corrosion models which are too conservative. Several other experiments are underway in the Swedish programme, therefore,

in order to define and quantify these effects, including study by means of power-bump tests of the possible migration of key nuclides to grain boundaries, and experiments designed to measure isotope-exchange processes between the solid and liquid phases. Only preliminary results are available from these experiments and they will be reported in a later publication.

Results are, however, available from the first year's corrosion of fuel/clad specimens from the Ringhals 1 BWR stringer rod. Figure 14 presents the gross γ scan of the rod shortly before commencement of the experiment together with the sampling plan for corrosion test specimens and fuel characterization. The local burnups along the rod, excluding the top end-pellets, were determined by means of γ spectrometric measurement of cesium nuclides in selected pellets, together with the mass spectrometric determination of burnup in the two inventory specimens. The values ranged from 21.2 MWd/kgU in the lower ceramographic specimen to 49.0 MWd/kgU at the top of the fuel column. Figure 15 shows a simplified irradiation history for the highest rated pellet over the 8 cycles in the Ringhals 1 reactor. The variation of local power with time was similar along the fuel column. The build-up of actinides along the rod was steeper than the burnup profile. Hence, the fuel column consisted of a series of fuel specimens of the same original fuel, which had experienced a wide range of burnups and linear heat ratings; and an even wider range of local α dose rates. The higher burnup specimens were expected to exhibit successive development of the characteristics of the fuel rim zone with respect to porosity and grain structure. An extensive fuel characterization programme has been performed on fuel pellets at three burnup levels, 21.2, 36.7 and 49.0 MWd/kgU. It has included measurement of radial profiles of α -activity, Pu/U ratio and selected fission product concentrations and a

detailed examination of fuel structure by optical and scanning electron microscopy. Although these results can only be briefly presented, the gradual development of the fuel rim structure, which was tentatively expected to have a significant effect on local corrosion properties, is illustrated in Figure 16. The photomicrographs show the fracture surface at the fuel periphery of the three characterized pellets. The specimen with the lowest burnup displayed predominantly transgranular fracture; whereas, in the 36.7 MWd/kgU specimen, the fission gas bubble network was so developed that intergranular fracture was observed. Bubble sites and particles (or subgrains) of recrystallized UO_2 can be observed on grain edges and faces. In the specimen with 49.0 MWd/kgU, the characteristics of the high burnup rim are already well established.

The corrosion tests on the 16 fuel/clad specimens dry-cut from the rod have been in progress since early 1990, and the results from the first year's exposure are now available. Thirteen of the segments were exposed to the reference groundwater (Table 1), 10 under oxic and 3 under anoxic conditions. The remaining 3 segments were corroded in DIW, 2 oxic and 1 anoxic.

The results were somewhat unexpected. Figures 17 and 18 present the cumulative release fractions for ^{137}Cs and ^{90}Sr as a function of cumulative leachant contact times, and of specimen burnup for the 10 specimens exposed to oxic groundwater. Figure 17 shows that the Instant Release Fraction for ^{137}Cs (28 day curve) varied along the rod from 0.4% to 0.75%, the release showing an almost step-wise increase at a burnup of 35 MWd/kgU. Even the ^{90}Sr release showed the same effect. From Figure 15, the fuel at this burnup experienced an average linear heat rating over the last 6 years of irradiation of only 10-11 kW/m. For exposure

times longer than 28 days, the release fractions for both nuclides attained a maximum at a burnup of about 44 MWd/kgU, but, surprisingly, at higher burnups decreased again. The same pattern was also shown by the release fractions for ^{99}Tc (not presented here), while uranium solubility behaviour was more or less uniform along the fuel column. It is possible that the increase in release fractions for Cs, Sr and Tc observed for fuel with a burnup of about 35 MWd/kgU is indeed related to linear power, i.e., migration to and enhanced concentration at grain boundaries due to fuel temperature gradients; although as seen above, the local power at this position in the rod was generally lower than one would expect to be required, on the basis of current fuel performance codes. However, the Instant Release Fractions for ^{137}Cs , that is, the solubilization of cesium already released from the fuel grains, show a contact time dependence during the first 28 days which varies along the rod (Figure 17). This suggests that leachant access to fuel surfaces can be at least a partial cause of the effect. Certainly, the unexpected decrease in release fractions for the specimens with the highest burnups, where peripheral porosity and α and β - γ dose rates to the leachant were also highest, must be due to other burnup-related structural effects. These experiments are still in progress and, hopefully, will generate data both from leachant analysis and fuel examination after corrosion which will permit a more satisfactory evaluation.

6 CONCLUSIONS

The actinide concentrations in the leach solutions have been found to be independent of contact time. A comparison between the experimental results and calculations supports the hypo-

thesis that the solution concentrations of actinides may be controlled by a U(IV)/U(VI) redox buffering.

The releases of cesium, strontium and technetium under oxidizing conditions show different trends. For cesium, there is a rapid release during the first few weeks, corresponding to the cesium which has migrated to the fuel/clad gap during irradiation in the reactor. After this release of the Instant Release Fraction, the release rates decrease fairly quickly but, with the data so far available, appear to level off with time. The strontium release rate is constant for the first few weeks, before showing about the same decreases with time as the values for cesium.

The strontium release rates are always lower than the cesium release rates and show no tendency to level off at longer contact times. Assuming that the strontium release rates at longer contact times represent the UO_2 alteration rate, a reasonable hypothesis is that the difference between the release behaviour of strontium and cesium reflects only the migration of cesium during irradiation. The early cesium release represents cesium released from the fuel grains to fuel/clad surfaces. The difference in the later stages of corrosion represent attack at grain boundaries enriched in migrated cesium.

The technetium release rate is between 10^{-5} and 10^{-6} /d. Unlike cesium and strontium, the technetium release rates is independent of contact time, such that after a few years it exceeds those for cesium and strontium. This indicates that technetium has a different source. Metallic inclusions of Mo, Tc, Ru, Rh and Pd have been observed in irradiated fuel. The release of technetium is probably controlled only by oxidation of these inclusions.

Under reducing or anoxic conditions, the releases of redox sensitive elements, such as uranium, plutonium and technetium are strongly affected, consistent with their lower solubilities at lower redox potentials. For cesium and strontium, there are only minor decreases in the release rates. The relatively high strontium release rate may be due to dissolution of fuel already partly oxidized. However, with the available data it is not possible to clearly establish which mechanisms are responsible for the observed release rate.

The characterization of the fuel specimens before and after corrosion has proven to be a powerful supplement to the solution analyses. Scanning electron microscopy has demonstrated enhanced corrosion at the fuel periphery, where the burnup and the actinide content are highest. Experiments performed on a stringer rod, with varying burnup along its length, has confirmed a dependence on corrosion rate on burnup. However, at the highest burnups, a decrease in the corrosion rate was observed. These experiments are still in progress and will, hopefully, generate data from both solution analysis and fuel examination after corrosion which will permit a more satisfactory evaluation.

ACKNOWLEDGEMENTS

The authors gratefully acknowledge the contributions of many of the staff of Studsvik's Hot Cell Laboratory, in particular, Ulla Britt Eklund, Ove Mattsson, Birgit Bivered and Leif Kjellberg. The EQ3/6 calculations were performed by Patrik Sellin, SKB, Stockholm. Thanks are also due to Dr Jordi Bruno, MBT, Barcelona, and professor Ingmar Grenthe, Royal Institute of

Technology, Stockholm, for critically reading the manuscript and for helpful discussions.

REFERENCES

- [1] Katayama, Y.B., Leaching of Irradiated LWR Fuel Pellets in Deionized and Typical Ground Water, Report No. BNWL-2057 (Battelle Pacific Northwest Laboratory, 1976).
- [2] Eklund, U.B. and Forsyth R.S., Leaching of Irradiated UO₂ Fuel, Report No. KBS-TR-70 (Swedish Nuclear Fuel and Waste Management Co, SKB, 1978).
- [3] Vandergraaf, T.T., Leaching of Irradiated UO₂ Fuel, Report TR-100 (Atomic Energy of Canada Limited, 1980).
- [4] Forsyth, R.S., Werme, L.O. and Bruno, J., J. Nucl. Mater., 138 (1986) 1.
- [5] Oversby, V.O. and Wilson, C.N., Derivation of a Waste Package Source Term for NNWSI from the Results of Laboratory Experiments, in: Mat. Res. Soc. Symp. Proc. Vol 50, 9th Symp. on Scientific Basis for Nuclear Waste Management, Stockholm, 1985, ed. L.O. Werme (Materials Research Society, Pittsburgh, PA, 1986) p. 337.
- [6] Wilson, C.N., Summary of Results from the Series 2 and 3 NNWSI Bars Fuel Tests, in: Mat. Res. Soc. Symp. Proc. Vol 112, 11th Symp. on Scientific Basis for Nuclear Waste Management, Boston, 1987, eds. M.J. Apted and R.E. Wes-

- terman (Materials Research Society, Pittsburgh, PA, 1988) p. 473.
- [7] Stroess-Gascoyne, S., Johnson, L.H., Beeley, P.A. and Sellinger, D.M., Dissolution of Used CANDU Fuel at Various Temperatures and Redox Conditions, in: Mat. Res. Soc. Symp. Proc. Vol 50, 9th Symp. on Scientific Basis for Nuclear Waste Management, Stockholm, 1985, ed. L.O. Werme (Materials Research Society, Pittsburgh, PA, 1986) p. 309.
- [8] Stroess-Gascoyne, S., Johnson, L.H., Tait, J.C. and Sellinger, D.M., Leaching of Whole, Defected CANDUTM Fuel in Saline Solutions Under Argon Pressure, in: Mat. Res. Soc. Symp. Proc. Vol 127, 12th Symp. on Scientific Basis for Nuclear Waste Management, Berlin, 1988, eds. W. Lutze and R.C. Ewing (Materials Research Society, Pittsburgh, PA, 1989) p. 301.
- [9] Johnson, L.H. and Shoesmith, D.W., Spent Fuel, in: Radioactive Wasteforms for the Future, eds. W. Lutze and R.C. Ewing, North-Holland Publ. Co., Amsterdam 1988) p. 635.
- [10] Forsyth, R.S. and Werme L.O., Corrosion Tests on Spent PWR Fuel in Synthetic Groundwater, Report TR 87-16 (Swedish Nuclear Fuel and Waste Management Co 1987)
- [11] Forsyth R.S., Spent Fuel Degradation, Mat. Res. Soc. Symp. Proc. Vol. 212, p. 177 (Materials Research Society, Pittsburgh, PA, 1991).
- [12] Forsyth R.S., The KBS UO₂ Leaching Programme, Report TR 83-26 (Swedish Nuclear Fuel and Waste Management Co 1983)

- [13] Wilson, C.N., Results from NNWSI Series 3. Bare Fuel Dissolution Tests, Report PNL-7170 (Pacific Northwest Laboratory, WA, USA, 1990)
- [14] Vernaz, E., Personal communication.
- [15] Wolery, T.J., Calculation of Chemical Equilibrium between Aqueous Solution and Minerals: The EQ3/6 Software Package, Report UCRL-52658 (Lawrence Livermore National Laboratory, Livermore CA, USA, 1979).
- [16] Puigdomènech, I. and Bruno, J., Modelling Uranium Solubilities in Aqueous Solutions: Validation of a Thermodynamic Data Base for the EQ3/6 Geochemical Codes, Report TR 88-21 (Swedish Nuclear Fuel and Waste Management Co, 1988).
- [17] Puigdomènech, I. and Bruno, J., Plutonium Solubilities, Report TR 91-04 (Swedish Nuclear Fuel and Waste Management Co, 1991).
- [18] Forsyth, R.S., Mattsson, O, and Schrire, D., Fission Product Concentration Profiles (Sr, Xe, Cs and Nd) at the Individual Grain Level in Power-Ramped LWR Fuel, Report TR 88-24 (Swedish Nuclear Fuel Waste Management Co 1988)
- [19] Thomas, L.E., Einziger, R.E., and Woodley, R.E. J.Nucl.Mater., 166 (1989) 243.
- [20] Forsyth, R.S., The Application of PIE Techniques to the Study of the Corrosion of Spent Oxide Fuel in Deep-Rock Groundwaters, Proceedings of the IAEA Technical Committee

Meeting on Postirradiation Examination Techniques for Reactor Fuel, Workington, England, 11-14 Sept. 1990.

- [21] Coquerelle, M. and Walker, C.T. UO₂ Irradiated at Extended Burnup: Fission Gas Release and Correlated Structural Features, Proceedings of the IAEA Technical Committee Meeting on Fuel Performance at High Burnup for Water Reactors, Nyköping, Sweden, 5-8 June, 1990.
- [22] Cunningham, M.E., Freshley, M.D., and Lanning, D.D. Development and Characteristics of the Rim Region in High Burnup UO₂ Fuel Pellets, Proceedings of the EMRS 1991 Fall Meeting: Symposium E Nuclear Materials for Fission Reactors, Strasbourg, France. 4-8 Nov. 1991.
- [23] Walker, C.T., Kameyama, T. and Kinoshita, M. Concerning the Microstructure Changes that Occur at the Surface of UO₂ Pellets on Irradiation to High Burnup, Ibid.
- [24] Forsyth, R.S., Eklund, U-B., Mattsson, O. and Schrire, D., Examination of the Surface Deposit on an Irradiated PWR Fuel Specimen subjected to Corrosion in Deionized Water, Report TR 90-04, (Swedish Nuclear Fuel and Waste Management Co. 1990)
- [25] Finch, R. and Ewing, R.C., Uraninite alteration in an oxidizing environment and its relevance to the disposal of spent nuclear fuel, Report TR 91-15 (Swedish Nuclear Fuel and Waste Management Co., 1991).
- [26] Bleiberg, M.L., Berman, R.M. and Lustman, B. in: Proc. on Radiation Damage in Reactor Materials, (IAEA, Vienna, Austria 1963) p. 319.

Table 2: Average plutonium concentrations (log mol/L) measured in fuel corrosion experiments in deionized water and in groundwater.

	DI Water	Groundwater
Sweden (SKB)	-7.9	-8.5 ^a -9.1 ^b -8.9 ^c
USA (YMP)		-8.4 ^d -9.1 ^e
France (CEA)		-7.5 ^f

- ^a average of all data.
^b average of contact times > 200 days only.
^c refers to ²³⁹Pu for very low burnup fuel. Pu content in the fuel is ca 1 % of the content in normal burnup fuel.
^d fuel from the H B Robinson power plant [12,13].
^e fuel from the Turkey Point power plant [12].
^f fast breeder fuel [14].

Table 3: Comparison of cumulative release fractions (1 year) under oxic and anoxic conditions.

Expt.	Burnup MWd/kgU	Redox	^{137}Cs	^{90}Sr	^{99}Tc	U	Pu
11-05	40.1	Oxic	$7.8 \cdot 10^{-3}$	$7.6 \cdot 10^{-4}$	$1.1 \cdot 10^{-3}$	$9.1 \cdot 10^{-5}$	$8.7 \cdot 10^{-6}$
11-06	41.4	Anoxic	$7.0 \cdot 10^{-3}$	$2.1 \cdot 10^{-4}$	$<2.1 \cdot 10^{-3}$	$<2.1 \cdot 10^{-6}$	ND
11-08	43.8	Oxic	$8.1 \cdot 10^{-3}$	$7.5 \cdot 10^{-4}$	$1.7 \cdot 10^{-3}$	$9.5 \cdot 10^{-5}$	$6.2 \cdot 10^{-6}$
11-09	44.9	Anoxic	$7.4 \cdot 10^{-3}$	$1.7 \cdot 10^{-4}$	$<2.3 \cdot 10^{-3}$	$<2.2 \cdot 10^{-6}$	ND
11-10	45.8	Oxic	$8.1 \cdot 10^{-3}$	$7.1 \cdot 10^{-4}$	$7.3 \cdot 10^{-3}$	$6.0 \cdot 10^{-5}$	$8.4 \cdot 10^{-6}$

Table 4: Comparison of ^{137}Cs fractional release rates (d^{-1}) under oxic and anoxic conditions.

Contact (d)	11-05 Oxic	11-06 Anoxic	11-08 Oxic	11-09 Anoxic	11-10 Oxic
7	$1.04 \cdot 10^{-3}$	$0.95 \cdot 10^{-3}$	$1.01 \cdot 10^{-3}$	$0.92 \cdot 10^{-3}$	$0.86 \cdot 10^{-3}$
21	$0.82 \cdot 10^{-5}$	$1.10 \cdot 10^{-5}$	$2.95 \cdot 10^{-5}$	$3.45 \cdot 10^{-5}$	$7.52 \cdot 10^{-5}$
63	$1.56 \cdot 10^{-6}$	$0.85 \cdot 10^{-6}$	$1.91 \cdot 10^{-6}$	$1.75 \cdot 10^{-6}$	$2.39 \cdot 10^{-6}$
91	$1.13 \cdot 10^{-6}$	$0.23 \cdot 10^{-6}$	$1.41 \cdot 10^{-6}$	$0.46 \cdot 10^{-6}$	$1.39 \cdot 10^{-6}$
182	$8.19 \cdot 10^{-7}$	$0.95 \cdot 10^{-7}$	$9.82 \cdot 10^{-7}$	$1.47 \cdot 10^{-7}$	$9.55 \cdot 10^{-7}$

Table 5: Comparison of ^{90}Sr fractional release rates (d^{-1}) under oxic and anoxic conditions.

Contact (d)	11-05 Oxic	11-06 Anoxic	11-08 Oxic	11-09 Anoxic	11-10 Oxic
7	$3.08 \cdot 10^{-5}$	$0.32 \cdot 10^{-5}$	$2.15 \cdot 10^{-5}$	$0.29 \cdot 10^{-5}$	$1.03 \cdot 10^{-5}$
21	$1.18 \cdot 10^{-5}$	$0.08 \cdot 10^{-5}$	$1.42 \cdot 10^{-5}$	$0.05 \cdot 10^{-5}$	$1.48 \cdot 10^{-5}$
63	$1.50 \cdot 10^{-6}$	$1.04 \cdot 10^{-6}$	$1.63 \cdot 10^{-6}$	$0.26 \cdot 10^{-6}$	$1.87 \cdot 10^{-6}$
91	$1.00 \cdot 10^{-6}$	$0.55 \cdot 10^{-6}$	$1.05 \cdot 10^{-6}$	$0.41 \cdot 10^{-6}$	$1.12 \cdot 10^{-6}$
182	$5.29 \cdot 10^{-7}$	$2.81 \cdot 10^{-7}$	$5.37 \cdot 10^{-7}$	$4.59 \cdot 10^{-7}$	$5.03 \cdot 10^{-7}$

Table 6: Cumulative release fractions for fuel fragments exposed under oxic conditions to corrosion in 4 mmol/L bicarbonate groundwater (3.25) and DIW (3.26).

Specimen	Leachant	Contact time (d)	Cumulative Release Fractions			
			U	¹³⁷ Cs	⁹⁰ Sr	⁹⁹ Tc
3.25	GW	1427	$2.2 \cdot 10^{-3}$	$1.2 \cdot 10^{-2}$	$3.3 \cdot 10^{-3}$	$4.7 \cdot 10^{-3}$
3.26	DIW	1521	$5.1 \cdot 10^{-6}$	$1.2 \cdot 10^{-2}$	$4.6 \cdot 10^{-3}$	$1.1 \cdot 10^{-3}$

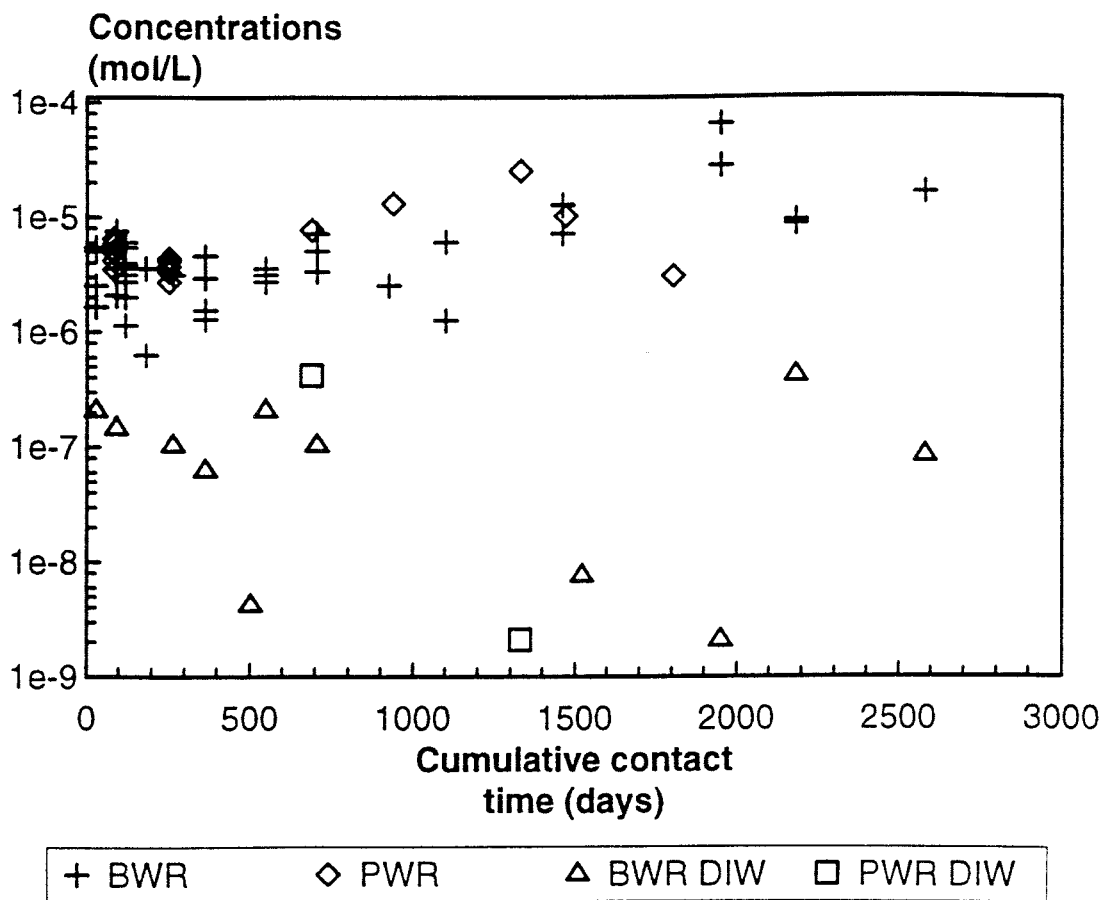


Fig. 1 Uranium concentration (oxic conditions) in DIW and synthetic groundwater as a function of cumulative contact time.

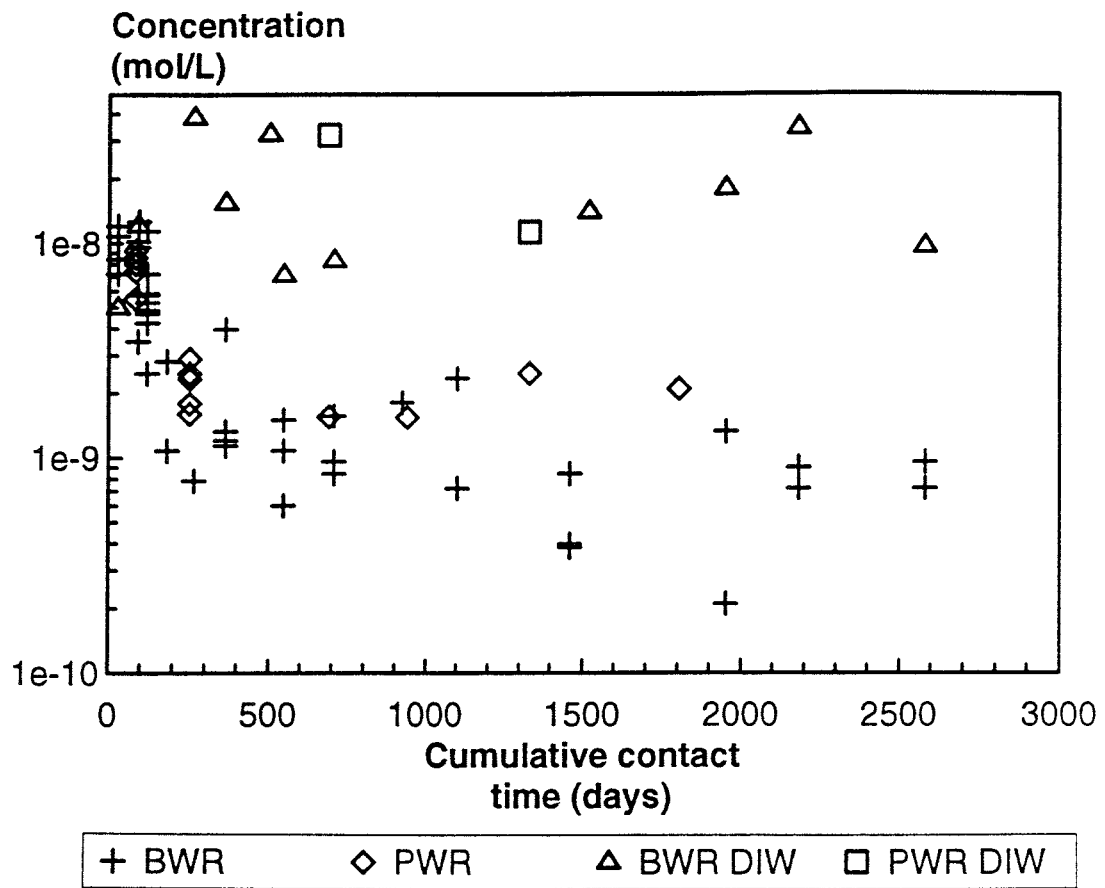


Fig. 2 Plutonium concentrations (oxic conditions) in DIW and synthetic groundwater as a function of cumulative contact time.

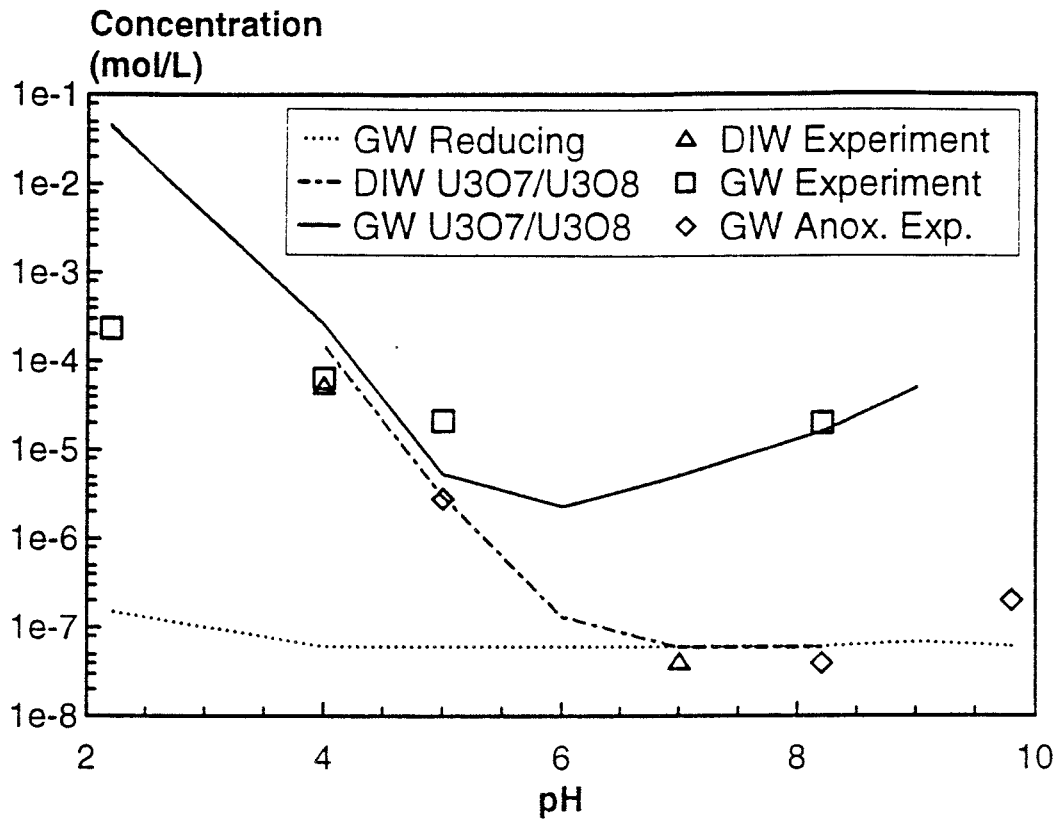


Fig. 3 Comparisons between calculated uranium solubilities and measured average concentrations as a function of pH.2

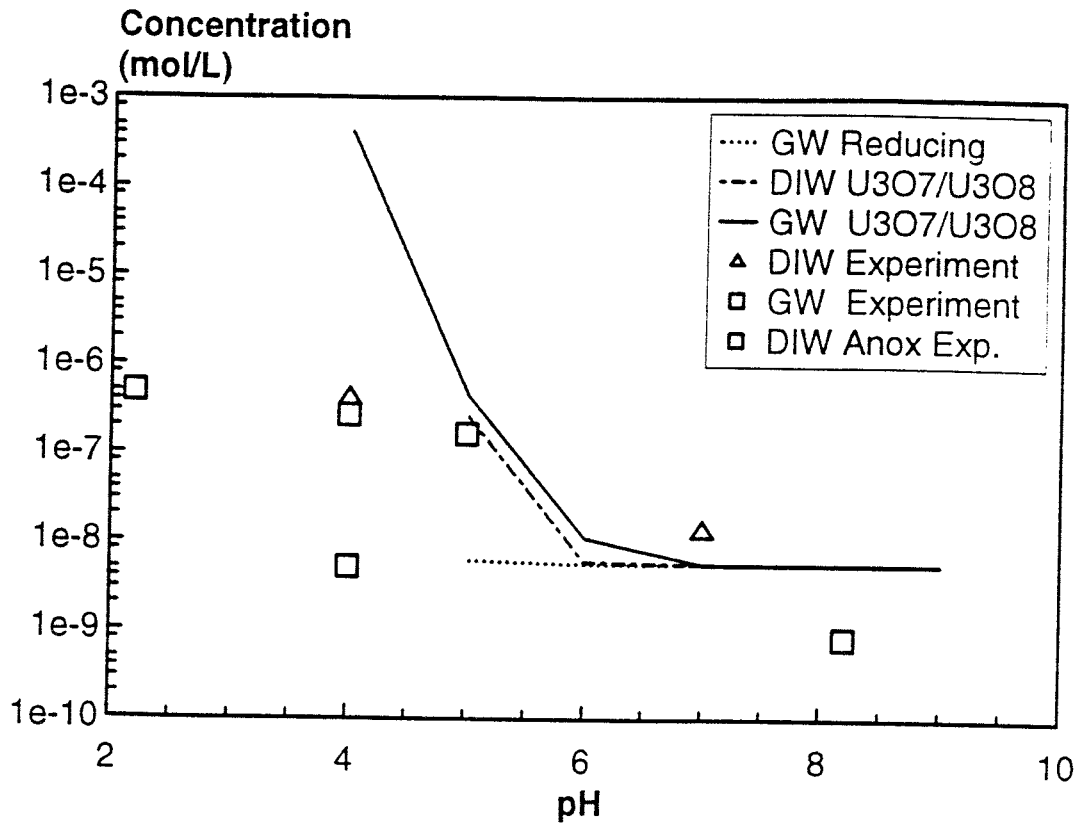


Fig 4. Comparisons between calculated plutonium solubilities and measured average concentrations as a function of pH.

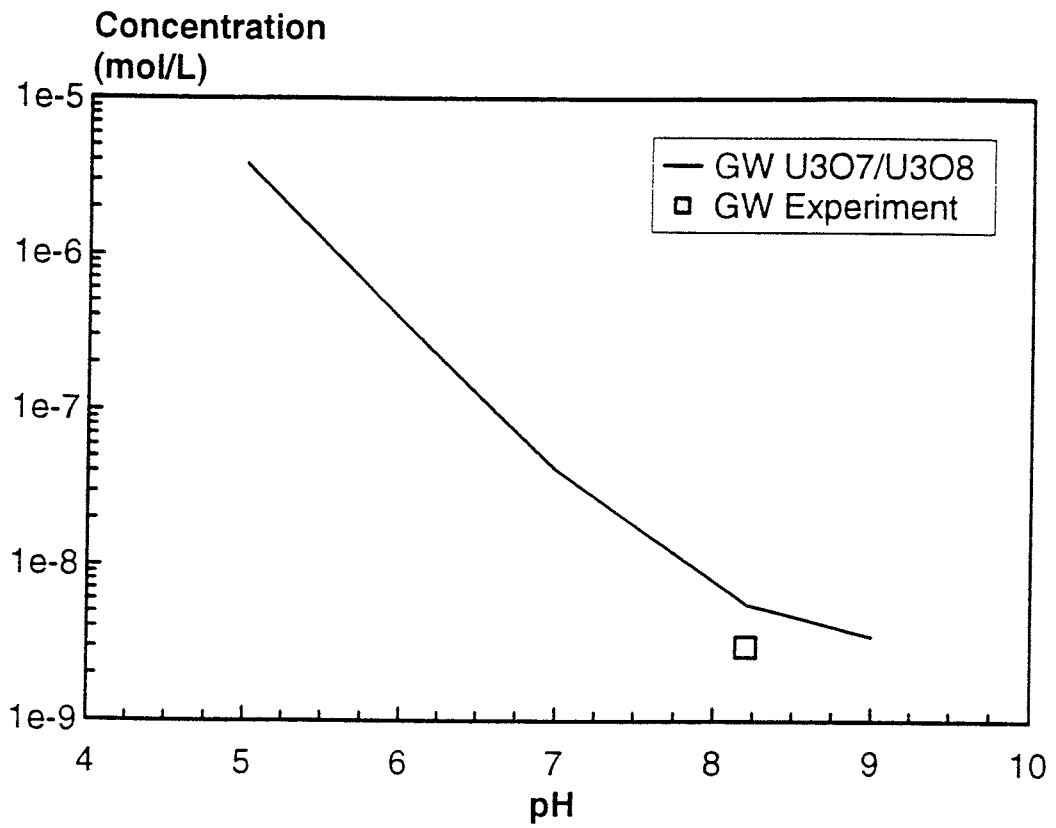


Fig. 5 Comparisons between calculated neptunium solubilities and measured average concentrations as a function of pH.

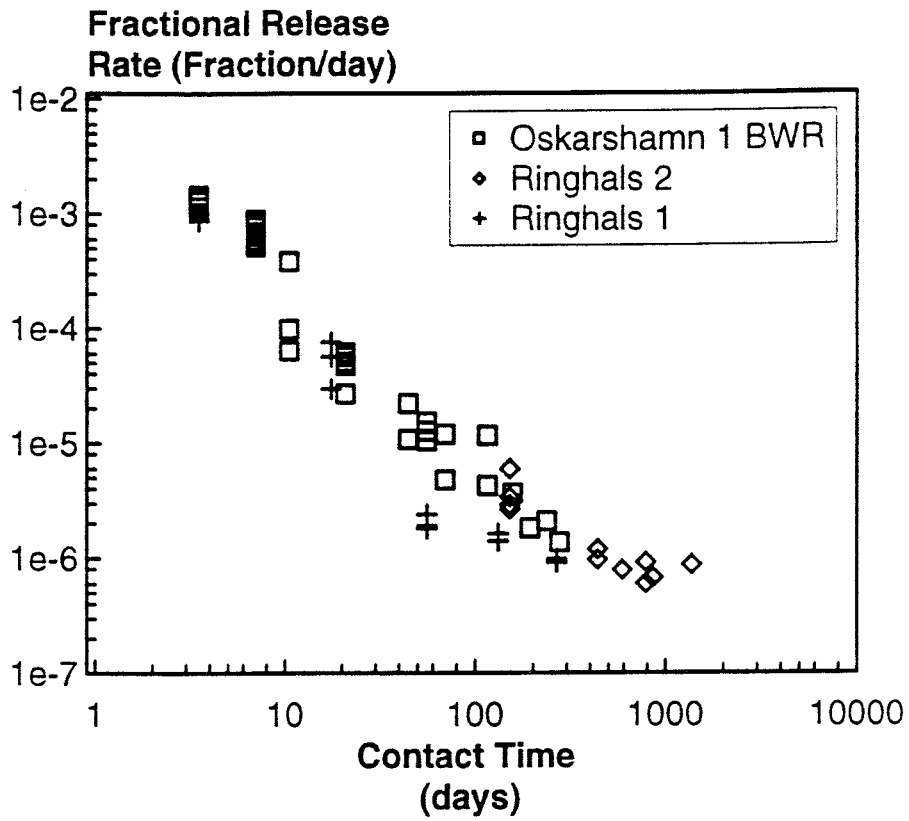


Fig. 6 Fractional release rates for Cs-137 under oxic conditions.

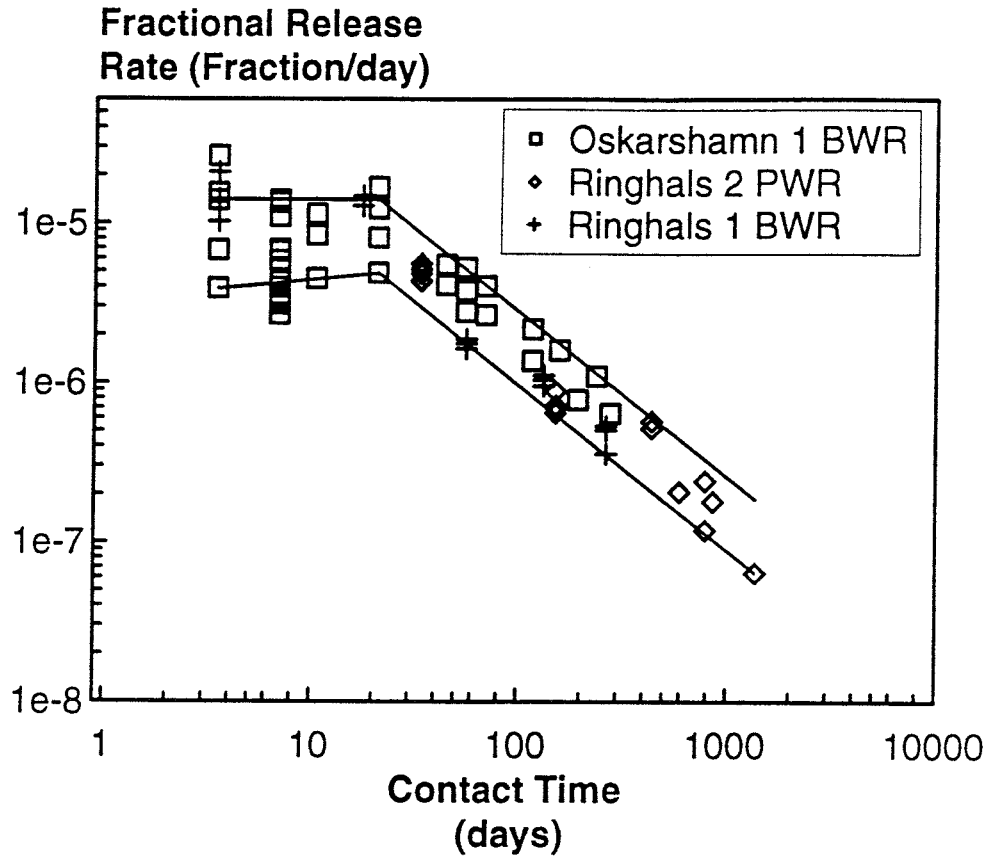


Fig. 7 Fractional release rates for Sr-90 under oxidic conditions.

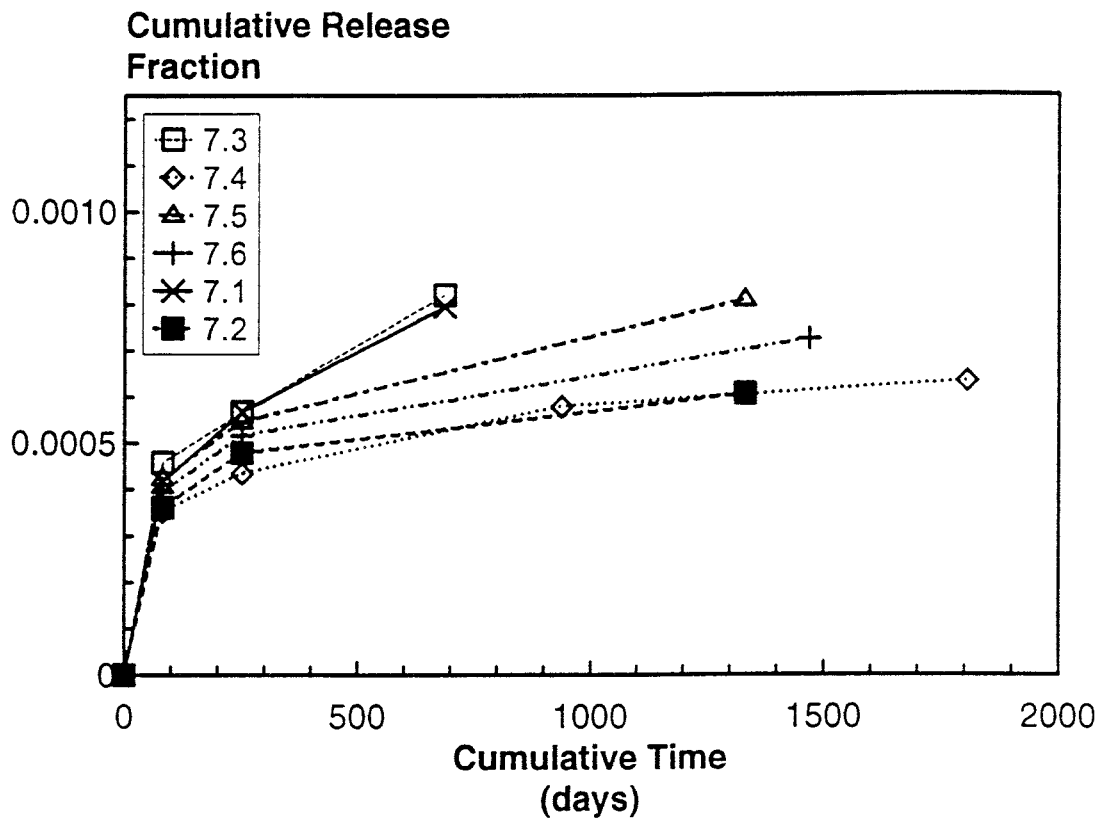


Fig. 8 Dependence of cumulative release fraction for Sr-90 on sampling position: PWR reference rod, oxidic conditions.

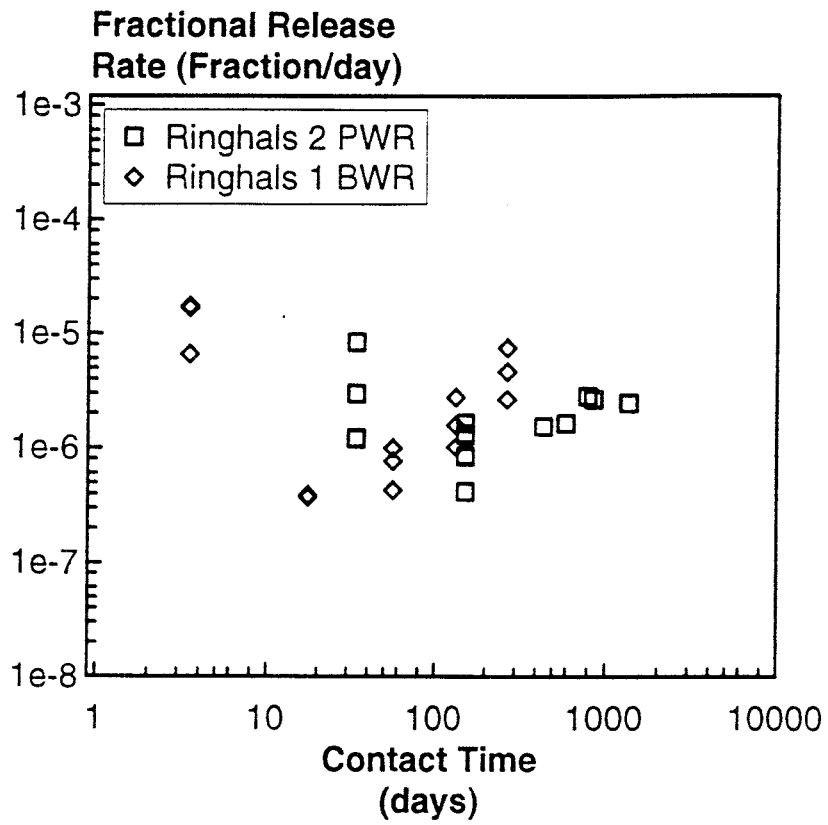


Fig. 9 Fractional release rates for Tc-99 under oxidic conditions.

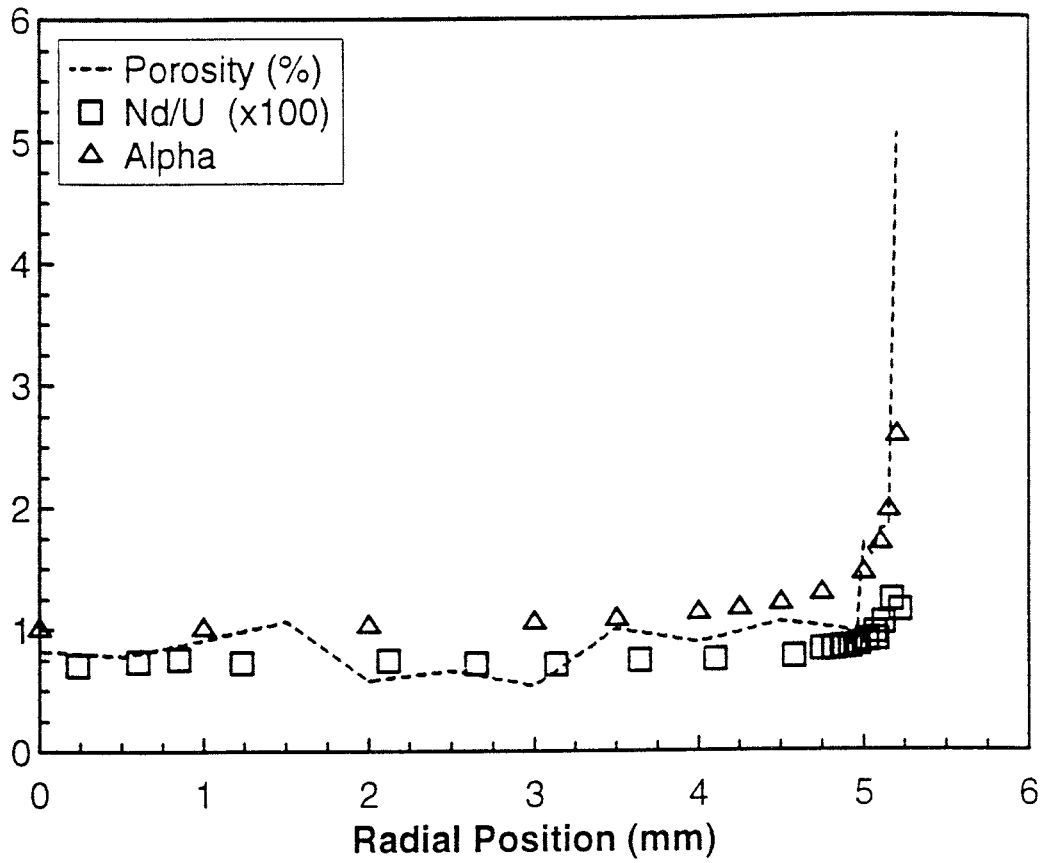


Fig. 10 Radial variation of fuel porosity, burnup and alpha activity in the Oskarshamn I BWR reference fuel.

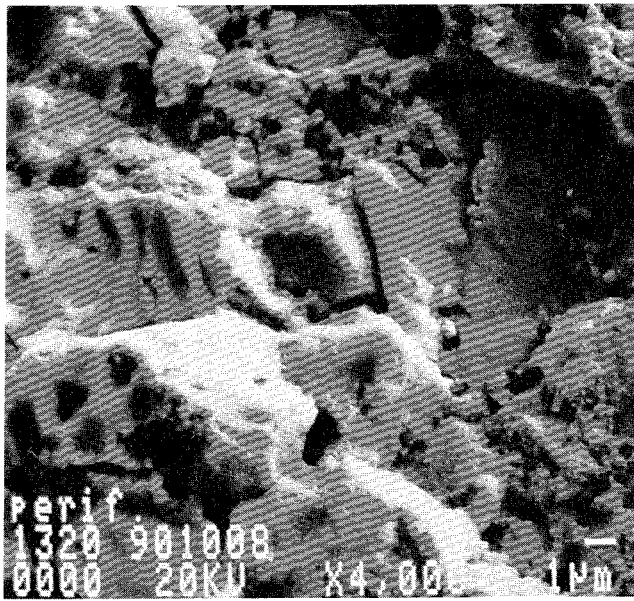


Fig. 11 Rim zone of BWR reference fuel (Oskarshamn 1)

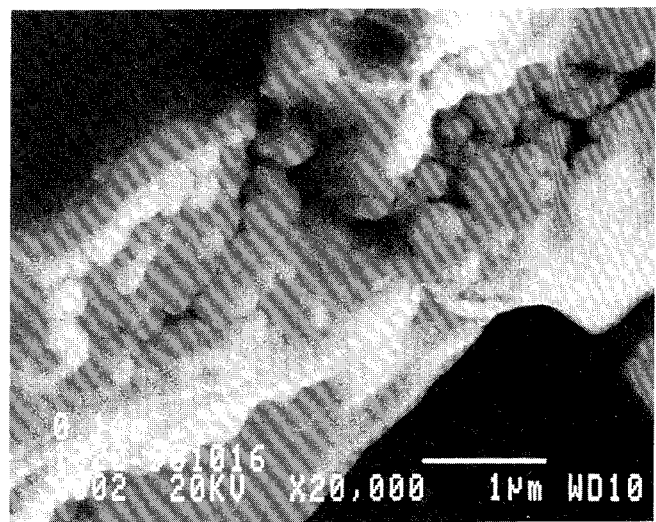
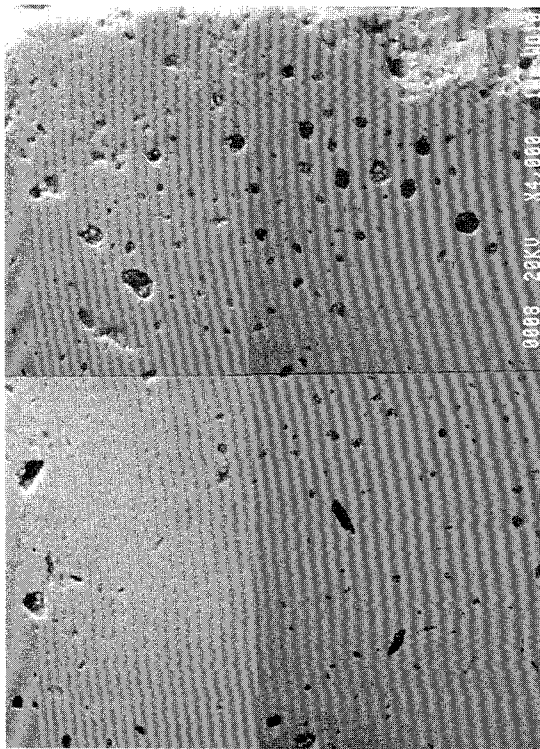
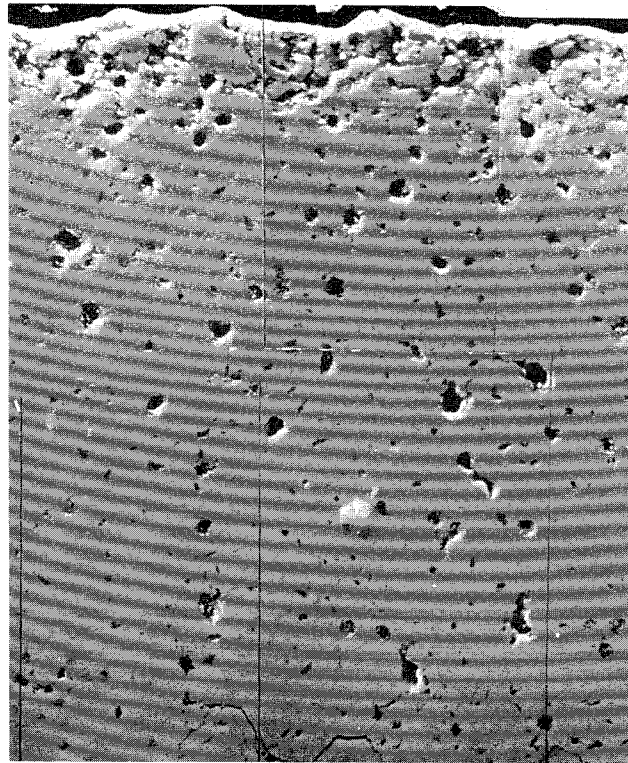


Fig. 12 Subgrains of UO₂ (?) 100 microns from the fuel periphery

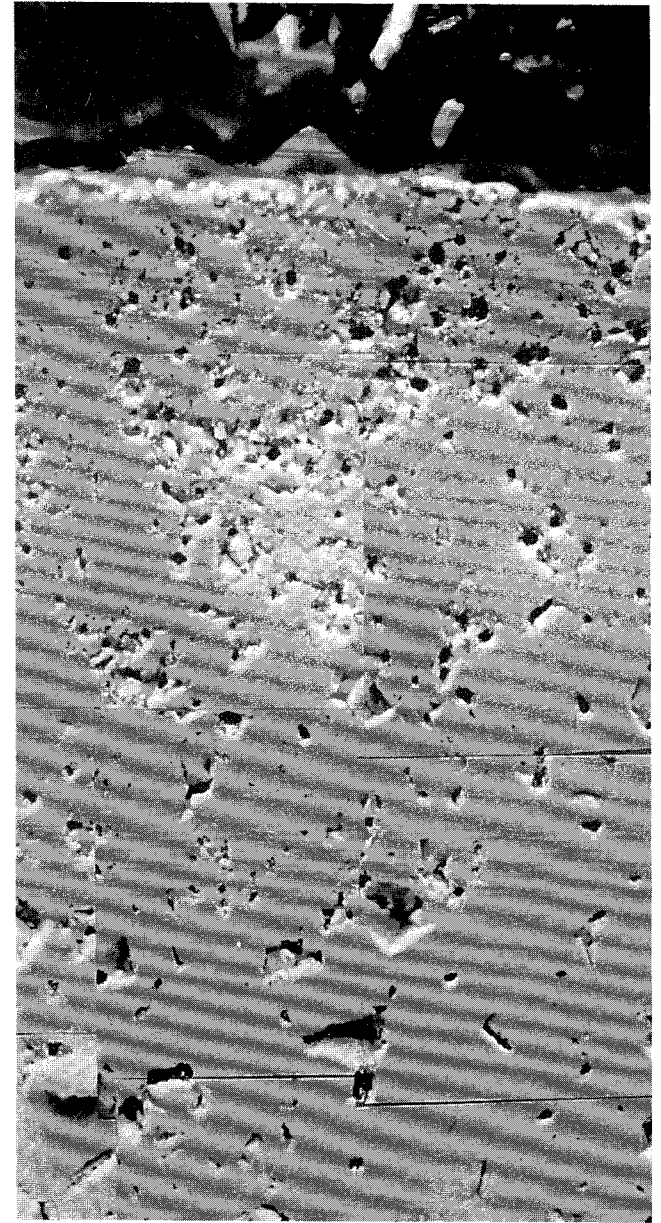


a



b

10 microns



c)

Fig. 13 Photomosaics of fuel rim zone
a) Uncorroded fuel, b) Expt. 3.25 (groundwater: 1427 d)
c) Expt. 3.26 (Deionized water: 1521 d)

C: CERAMOGRAPHY, EPMA, AUTORADIOGRAPHY
 I: INVENTORY DETERMINATION
 D: FUEL DENSITY DETERMINATION

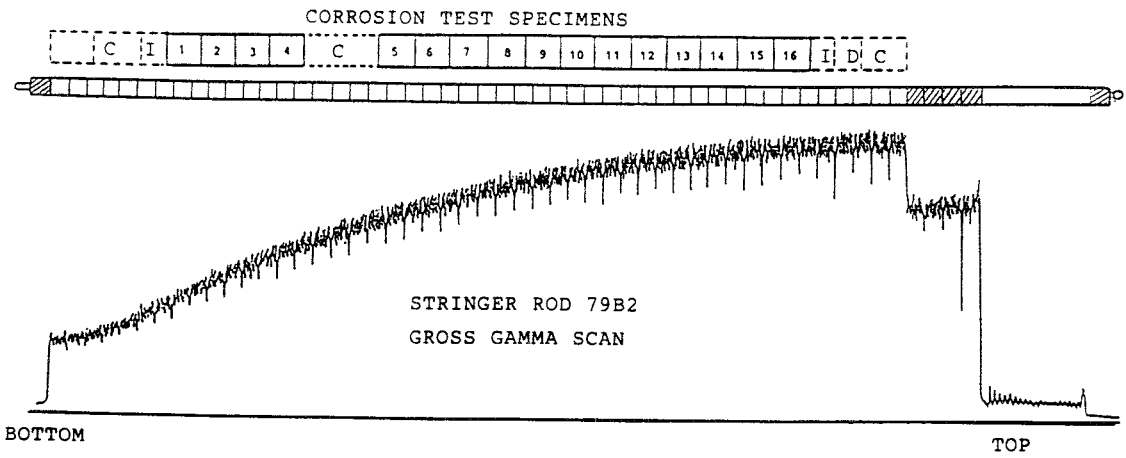


Fig. 14 Ringhals I BWR stringer rod: gross gamma scan and sampling plan.

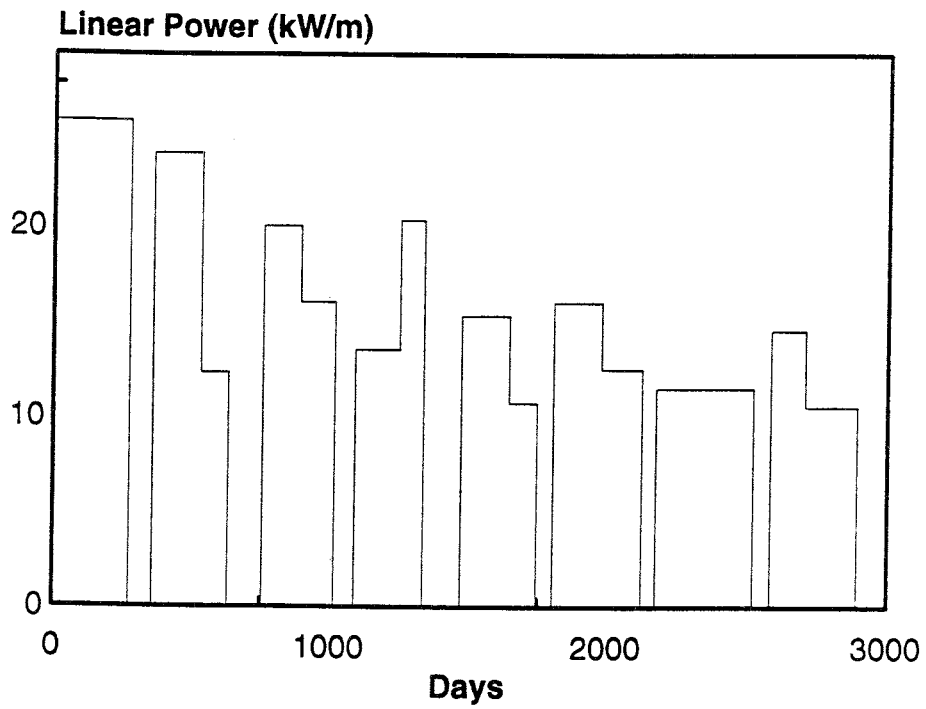
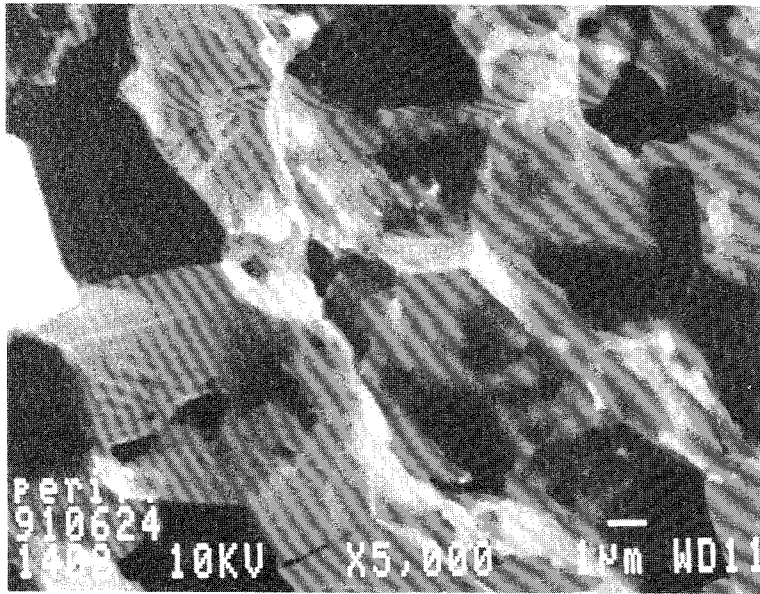
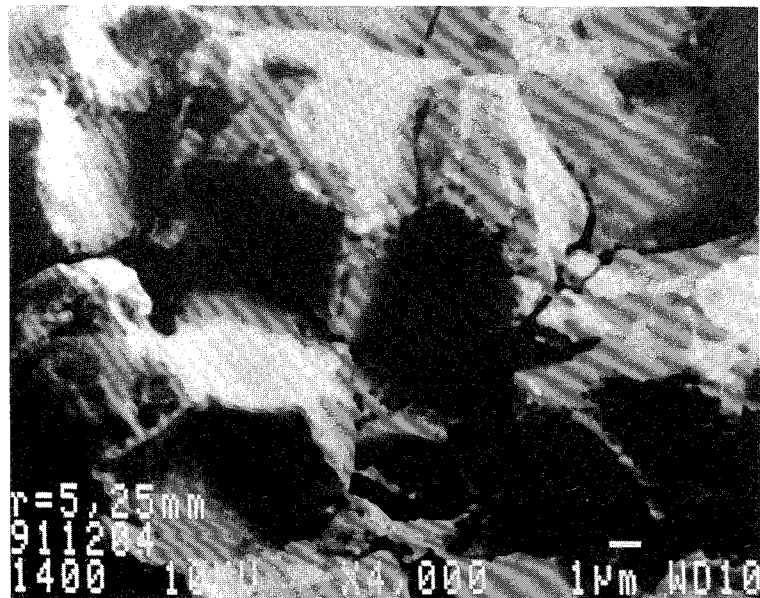


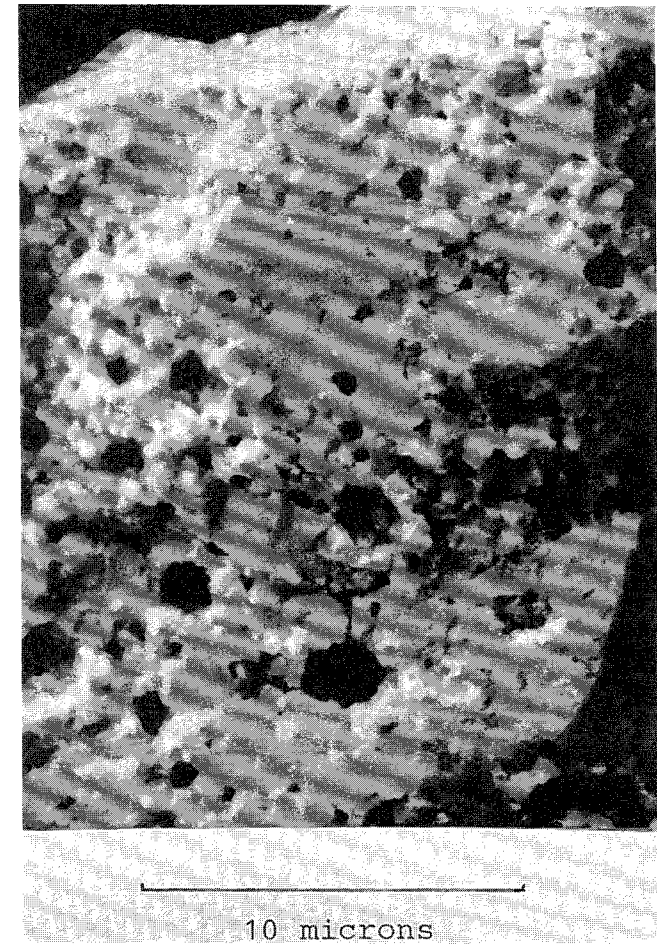
Fig 15. Ringhals I BWR stringer rod: simplified irradiation history.



a)



b)



c)

Fig 16. Ringhals I stringer rod: fuel fracture surface at pellet periphery.

- a) Bulk burnup 21.2 MWd/kg U.
- b) 36.7 MWd/kg U.
- c) 49.0 MWd/kg U.

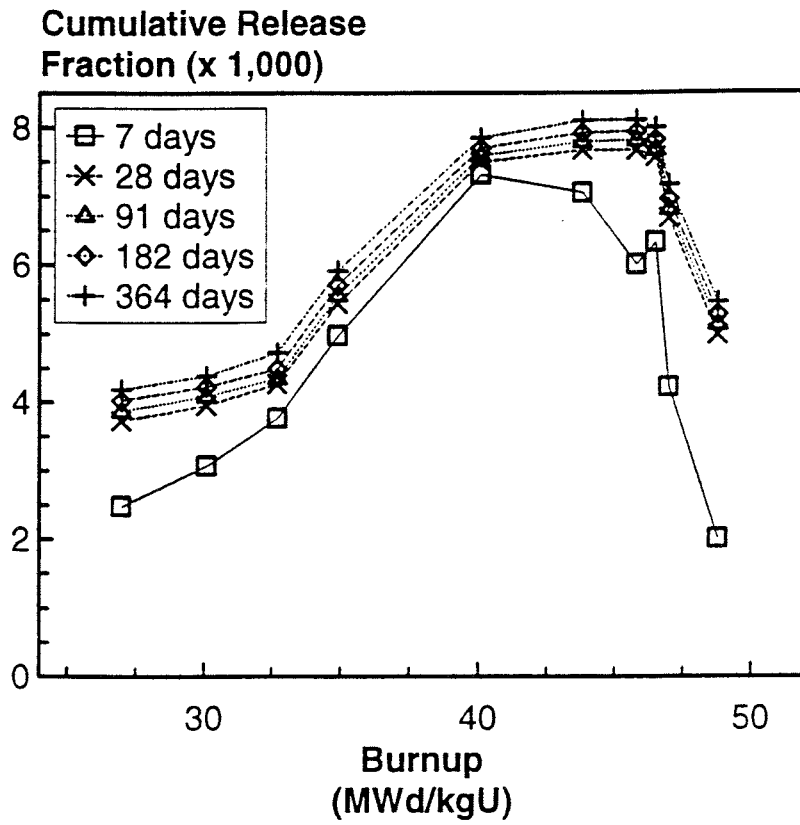


Fig. 17 Cumulative release fractions for Cs-137 as a function of specimen burnup (groundwater: oxic conditions).

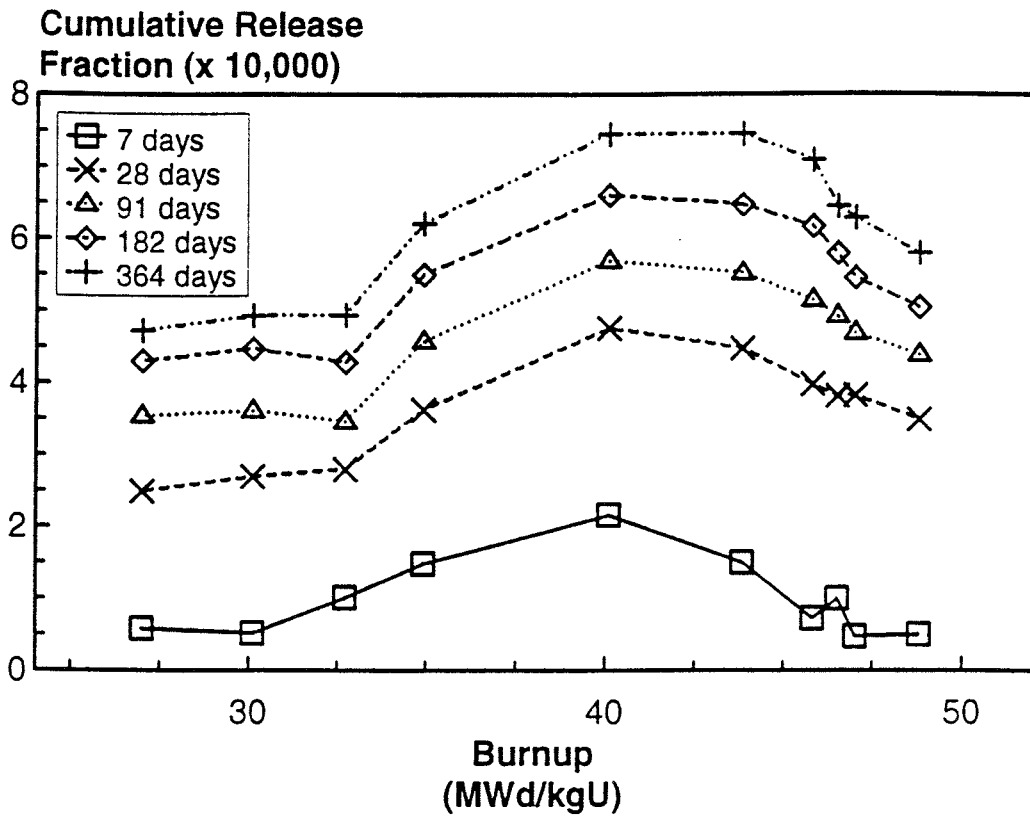


Fig. 18 Cumulative release fractions for Sr-90 as a function of specimen burnup (groundwater: oxic conditions).

List of SKB reports

Annual Reports

1977-78

TR 121

KBS Technical Reports 1 – 120

Summaries

Stockholm, May 1979

1979

TR 79-28

The KBS Annual Report 1979

KBS Technical Reports 79-01 – 79-27

Summaries

Stockholm, March 1980

1980

TR 80-26

The KBS Annual Report 1980

KBS Technical Reports 80-01 – 80-25

Summaries

Stockholm, March 1981

1981

TR 81-17

The KBS Annual Report 1981

KBS Technical Reports 81-01 – 81-16

Summaries

Stockholm, April 1982

1982

TR 82-28

The KBS Annual Report 1982

KBS Technical Reports 82-01 – 82-27

Summaries

Stockholm, July 1983

1983

TR 83-77

The KBS Annual Report 1983

KBS Technical Reports 83-01 – 83-76

Summaries

Stockholm, June 1984

1984

TR 85-01

Annual Research and Development Report 1984

Including Summaries of Technical Reports Issued during 1984. (Technical Reports 84-01 – 84-19)

Stockholm, June 1985

1985

TR 85-20

Annual Research and Development Report 1985

Including Summaries of Technical Reports Issued during 1985. (Technical Reports 85-01 – 85-19)

Stockholm, May 1986

1986

TR 86-31

SKB Annual Report 1986

Including Summaries of Technical Reports Issued during 1986

Stockholm, May 1987

1987

TR 87-33

SKB Annual Report 1987

Including Summaries of Technical Reports Issued during 1987

Stockholm, May 1988

1988

TR 88-32

SKB Annual Report 1988

Including Summaries of Technical Reports Issued during 1988

Stockholm, May 1989

1989

TR 89-40

SKB Annual Report 1989

Including Summaries of Technical Reports Issued during 1989

Stockholm, May 1990

1990

TR 90-46

SKB Annual Report 1990

Including Summaries of Technical Reports Issued during 1990

Stockholm, May 1991

Technical Reports

List of SKB Technical Reports 1991

TR 91-01

Description of geological data in SKB's database GEOTAB Version 2

Stefan Sehlstedt, Tomas Stark

SGAB, Luleå

January 1991

TR 91-02

Description of geophysical data in SKB database GEOTAB Version 2

Stefan Sehlstedt

SGAB, Luleå

January 1991

TR 91-03

1. The application of PIE techniques to the study of the corrosion of spent oxide fuel in deep-rock ground waters

2. Spent fuel degradation

R S Forsyth

Studsvik Nuclear

January 1991

TR 91-09

Long term sampling and measuring program. Joint report for 1987, 1988 and 1989. Within the project: Fallout studies in the Gideå and Finnsjö areas after the Chernobyl accident in 1986

Thomas Ittner

SGAB, Uppsala

December 1990

TR 91-04

Plutonium solubilities

I Puigdomènech¹, J Bruno²

¹Environmental Services, Studsvik Nuclear, Nyköping, Sweden

²MBT Tecnologia Ambiental, CENT, Cerdanyola, Spain

February 1991

TR 91-10

Sealing of rock joints by induced calcite precipitation. A case study from Bergforsen hydro power plant

Eva Hakami¹, Anders Ekstav², Ulf Qvarfort²

¹Vattenfall HydroPower AB

²Golder Geosystem AB

January 1991

TR 91-05

Description of tracer data in the SKB database GEOTAB

SGAB, Luleå

April, 1991

TR 91-11

Impact from the disturbed zone on nuclide migration – a radioactive waste repository study

Akke Bengtsson¹, Bertil Grundfelt¹,

Anders Markström¹, Anders Rasmuson²

¹KEMAKTA Konsult AB

²Chalmers Institute of Technology

January 1991

TR 91-06

Description of background data in the SKB database GEOTAB

Version 2

Ebbe Eriksson, Stefan Sehlstedt

SGAB, Luleå

March 1991

TR 91-12

Numerical groundwater flow calculations at the Finnsjön site

Björn Lindbom, Anders Boghammar,

Hans Lindberg, Jan Bjelkås

KEMAKTA Consultants Co, Stockholm

February 1991

TR 91-07

Description of hydrogeological data in the SKB's database GEOTAB

Version 2

Margareta Gerlach (ed.)

Mark Radon Miljö MRM Konsult AB,

Luleå

December 1991

TR 91-13

Discrete fracture modelling of the Finnsjön rock mass

Phase 1 feasibility study

J E Geier, C-L Axelsson

Golder Geosystem AB, Uppsala

March 1991

TR 91-14

Channel widths

Kai Palmqvist, Marianne Lindström

BERGAB-Berggeologiska Undersökningar AB

February 1991

TR 91-08

Overview of geologic and geohydrologic conditions at the Finnsjön site and its surroundings

Kaj Ahlbom¹, Sven Tirén²

¹Conterra AB

²Sveriges Geologiska AB

January 1991

TR 91-15

Uraninite alteration in an oxidizing environment and its relevance to the disposal of spent nuclear fuel

Robert Finch, Rodney Ewing

Department of Geology, University of New Mexico

December 1990

TR 91-16
Porosity, sorption and diffusivity data compiled for the SKB 91 study
Fredrik Brandberg, Kristina Skagius
Kemakta Consultants Co, Stockholm
April 1991

TR 91-17
Seismically deformed sediments in the Lansjärv area, Northern Sweden
Robert Lagerbäck
May 1991

TR 91-18
Numerical inversion of Laplace transforms using integration and convergence acceleration
Sven-Åke Gustafson
Rogaland University, Stavanger, Norway
May 1991

TR 91-19
NEAR21 - A near field radionuclide migration code for use with the PROPER package
Sven Norman¹, Nils Kjellbert²
¹Starprog AB
²SKB AB
April 1991

TR 91-20
Äspö Hard Rock Laboratory. Overview of the investigations 1986-1990
R Stanfors, M Erlström, I Markström
June 1991

TR 91-21
Äspö Hard Rock Laboratory. Field investigation methodology and instruments used in the pre-investigation phase, 1986-1990
K-E Almén, O Zellman
June 1991

TR 91-22
Äspö Hard Rock Laboratory. Evaluation and conceptual modelling based on the pre-investigations 1986-1990
P Wikberg, G Gustafson, I Rhén, R Stanfors
June 1991

TR 91-23
Äspö Hard Rock Laboratory. Predictions prior to excavation and the process of their validation
Gunnar Gustafson, Magnus Liedholm, Ingvar Rhén, Roy Stanfors, Peter Wikberg
June 1991

TR 91-24
Hydrogeological conditions in the Finnsjön area. Compilation of data and conceptual model
Jan-Erik Andersson, Rune Nordqvist, Göran Nyberg, John Smellie, Sven Tirén
February 1991

TR 91-25
The role of the disturbed rock zone in radioactive waste repository safety and performance assessment. A topical discussion and international overview.
Anders Winberg
June 1991

TR 91-26
Testing of parameter averaging techniques for far-field migration calculations using FARF31 with varying velocity.
Akke Bengtsson¹, Anders Boghammar¹, Bertil Grundfelt¹, Anders Rasmuson²
¹KEMAKTA Consultants Co
²Chalmers Institute of Technology

TR 91-27
Verification of HYDRASTAR. A code for stochastic continuum simulation of groundwater flow
Sven Norman
Starprog AB
July 1991

TR 91-28
Radionuclide content in surface and groundwater transformed into breakthrough curves. A Chernobyl fallout study in an forested area in Northern Sweden
Thomas Ittner, Erik Gustafsson, Rune Nordqvist
SGAB, Uppsala
June 1991

TR 91-29
Soil map, area and volume calculations in Orrmyrberget catchment basin at Gideå, Northern Sweden
Thomas Ittner, P-T Tammela, Erik Gustafsson
SGAB, Uppsala
June 1991

TR 91-30

A resistance network model for radionuclide transport into the near field surrounding a repository for nuclear waste (SKB, Near Field Model 91)

Lennart Nilsson, Luis Moreno, Ivars Neretnieks, Leonardo Romero
Department of Chemical Engineering,
Royal Institute of Technology, Stockholm
June 1991

TR 91-31

Near field studies within the SKB 91 project

Hans Widén, Akke Bengtsson, Bertil Grundfelt
Kemakta Consultants AB, Stockholm
June 1991

TR 91-32

SKB/TVO Ice age scenario

Kaj Ahlbom¹, Timo Äikäs², Lars O. Ericsson³
¹Conterra AB
²Teollisuuden Voima Oy (TVO)
³Svensk Kärnbränslehantering AB (SKB)
June 1991

TR 91-33

Transient nuclide release through the bentonite barrier - SKB 91

Akke Bengtsson, Hans Widén
Kemakta Konsult AB
May 1991

TR 91-34

SIMFUEL dissolution studies in granitic groundwater

I Casas¹, A Sandino², M S Caceci¹, J Bruno¹, K Ollila³
¹MBT Tecnologia Ambiental, CENT, Cerdanyola, Spain
²KTH, Dpt. of Inorganic Chemistry, Stockholm, Sweden
³VTT, Tech. Res. Center of Finland, Espoo, Finland
September 1991

TR 91-35

Storage of nuclear waste in long boreholes

Håkan Sandstedt¹, Curt Wichmann¹, Roland Pusch², Lennart Börgesson², Bengt Lönnerberg³
¹Tyréns
²Clay Technology AB
³ABB Atom
August 1991

TR 91-36

Tentative outline and siting of a repository for spent nuclear fuel at the Finnsjön site. SKB 91 reference concept

Lars Ageskog, Kjell Sjödin
VBB VIAK
September 1991

TR 91-37

Creep of OFHC and silver copper at simulated final repository canister-service conditions

Pertti Auerkari, Heikki Leinonen, Stefan Sandlin
VTT, Metals Laboratory, Finland
September 1991

TR 91-38

Production methods and costs of oxygen free copper canisters for nuclear waste disposal

Hannu Rajainmäki, Mikko Nieminen, Lenni Laakso
Outokumpu Poricopper Oy, Finland
June 1991

TR 91-39

The reducibility of sulphuric acid and sulphate in aqueous solution (translated from German)

Rolf Grauer
Paul Scherrer Institute, Switzerland
July 1990

TR 91-40

Interaction between geosphere and biosphere in lake sediments

Björn Sundblad, Ignasi Puigdomenech, Lena Mathiasson
December 1990

TR 91-41

Individual doses from radionuclides released to the Baltic coast

Ulla Bergström, Sture Nordlinder
Studsvik AB
May 1991

TR 91-42

Sensitivity analysis of the groundwater flow at the Finnsjön study site

Yung-Bing Bao, Roger Thunvik
Dept. Land and Water Resources,
Royal Institute of Technology, Stockholm, Sweden
September 1991

TR 91-43
SKB - PNC
Development of tunnel radar antennas
Lars Falk
ABEM, Uppsala, Sweden
July 1991

TR 91-44
Fluid and solute transport in a network of channels
Luis Moreno, Ivars Neretnieks
Department of Chemical Engineering,
Royal Institute of Technology, Stockholm, Sweden
September 1991

TR 91-45
The implications of soil acidification on a future HLNW repository.
Part I: The effects of increased weathering, erosion and deforestation
Josefa Nebot, Jordi Bruno
MBT Tecnología Ambiental, Cerdanyola, Spain
July 1991

TR 91-46
Some mechanisms which may reduce radiolysis
Ivars Neretnieks, Mostapha Faghihi
Department of Chemical Engineering, Royal
Institute of Technology, Stockholm, Sweden
August 1991

TR 91-47
On the interaction of granite with Tc(IV) and Tc(VII) in aqueous solution
Trygve E Eriksen, Daqing Cui
Royal Institute of Technology, Department of
Nuclear Chemistry, Stockholm, Sweden
October 1991

TR 91-48
A compartment model for solute transport in the near field of a repository for radioactive waste (Calculations for Pu-239)
Leonardo Romero, Luis Moreno, Ivars Neretnieks
Department of Chemical Engineering, Royal
Institute of Technology, Stockholm, Sweden
October 1991

TR 91-49
Description of transport pathways in a KBS-3 type repository
Roland Pusch¹, Ivars Neretnieks², Patrik Sellin³
¹ Clay Technology AB, Lund
² The Royal Institute of Technology Department of
Chemical Engineering, Stockholm
³ Swedish Nuclear Fuel and Waste Manage-
ment Co (SKB), Stockholm
December 1991

TR 91-50
Concentrations of particulate matter and humic substances in deep groundwaters and estimated effects on the adsorption and transport of radionuclides
Bert Allard¹, Fred Karlsson², Ivars Neretnieks³
¹ Department of Water and Environmental Studies,
University of Linköping, Sweden
² Swedish Nuclear Fuel and Waste Management
Company, SKB, Stockholm, Sweden
³ Department of Chemical Engineering, Royal
Institute of Technology, Stockholm, Sweden
November 1991

TR 91-51
Gideå study site. Scope of activities and main results
Kaj Ahlbom¹, Jan-Erik Andersson²,
Rune Nordqvist², Christer Ljunggren², Sven Tirén²,
Clifford Voss³
¹ Conterra AB
² Geosigma AB
³ U.S. Geological Survey
October 1991

TR 91-52
Fjällveden study site. Scope of activities and main results
Kaj Ahlbom¹, Jan-Erik Andersson²,
Rune Nordqvist², Christer Ljunggren², Sven Tirén²,
Clifford Voss³
¹ Conterra AB
² Geosigma AB
³ U.S. Geological Survey
October 1991

TR 91-53
Impact of a repository on permafrost development during glaciation advance
Per Vallander, Jan Eurenium
VBB VIAK AB
December 1991

TR 91-54

Hydraulic evaluation of the groundwater conditions at Finnsjön. The effects on dilution in a domestic well

C-L Axelsson¹, J Byström¹, Å Eriksson¹,
J Holmén¹, H M Haitjema²

¹Golder Geosystem AB, Uppsala, Sweden

²School of Public and Environmental Affairs,
Indiana University, Bloomington, Indiana, USA

September 1991

TR 91-58

Exploratory calculations concerning the influence of glaciation and permafrost on the groundwater flow system, and an initial study of permafrost influence at the Finnsjön site - an SKB 91 study

Björn Lindbom, Anders Boghammar

Kemakta Konsult AB, Stockholm

December 1991

TR 91-55

Redox capacity of crystalline rocks. Laboratory studies under 100 bar oxygen gas pressure

Veijo Pirhonen, Petteri Pitkänen

Technical Research Center of Finland

December 1991

TR 91-59

Proceedings from the technical workshop on near-field performance assessment for high-level waste held in Madrid October 15-17, 1990

Patrik Sellin¹, Mick Apted², José Gago³ (editors)

¹SKB, Stockholm, Sweden

²Intera, Denver, USA

³ENRESA, Madrid, Spain

December 1991

TR 91-56

Microbes in crystalline bedrock. Assimilation of CO₂ and introduced organic compounds by bacterial populations in groundwater from deep crystalline bedrock at Laxemar and Stripa

Karsten Pedersen, Susanne Ekendahl,

Johanna Arlinger

Department of General and Marine Microbiology,

University of Göteborg, Göteborg, Sweden

December 1991

TR 91-57

The groundwater circulation in the Finnsjö area - the impact of density gradients

Part A: Saline groundwater at the Finnsjö site and its surroundings

Kaj Ahlbom

CONTERRA AB

Part B: A numerical study of the combined effects of salinity gradients, temperature gradients and fracture zones

Urban Svensson

CFE AB

Part C: A three-dimensional numerical model of groundwater flow and salinity distribution in the Finnsjö area

Urban Svensson

CFE AB

November 1991